

Transversal folding in Himalaya foothill ranges In memory of Frank HORVÁTH

Motto: Frank's favourite joke: "An Earth scientist is falling off from the 100th floor of a skyscraper. At the third floor he says: "So far, so good". All his observations were right. But the predictive power..."

CSONTOS, László¹, DUNKL, István², VAKARCS, Gábor³, ABBASI, Abid H.³

¹MOL Nyrt, lcsontos@mol.hu; orcid: 0000-0002-0723-4673

²Sedimentology and Environmental Geology, Geozentrum, University of Göttingen; istvan.dunkl@geo.uni-goettingen.de

³MOL Pakistan, gabor.vakarcs@molpakistan.com; abid.abbasi@molpakistan.com

Harántirányú redők a Himalája előhegyeiben

Összefoglalás

Az észak-pakisztáni Himalája Fő frontális feltolódási (MFT) és Fő határfeltolódási (MBT) zónája több szintaxist (beöblösödést) tartalmaz. Ezek mentén az általános K–Ny-i csapású feltolódásokat nagyjából É–D-i csapású szakaszok kötik össze, amelyeket a közvélekedés eltolódásos jellegű oldalsó rámpáknak tart. E feltolódási zónák mentén két területet: a Kalabagh város környékét és az Islamabadtól keletre–délkeletre fekvőt mutatjuk be, amelyek szerkezeti elemzése ezt a vélekedést megkérdőjelezi. Az itt bemutatott szeizmikus szelvények alapján a javasolt oldalsó rámpák nem észlelhetők, ellenben É–D-i tengelyű redőket és keleti vagy nyugati vergenciájú feltolódásokat térképezhetünk, melyek érintik a paleo-meozoos kőzeteket és az oligo-mio-pliocén molasszt is.

A Surghar-hegység ÉK-i sarkát egymást váltó pikkelyek alkotják, amelyeknek kiemelkedő kambriumi–eocén magja van a kissé lenyesett miocén molassz alatt. Ezek az egymást váltó szerkezetek egy széles zónában dél felé legörbülnek. Ebben a zónában kulisszaszerű transzpressziós Riedelek, kulisszaszerű redők és délre görbülő korábbi feltolódások találhatók. Az összes ilyen szerkezet egy széles képlékeny jobbos nyírási zónaként értelmezhető, mely deformálja a korábban kialakult É–D-i tengelyű redőket és keleti vergenciájú feltolódásokat is (de a korábban javasolt Kalabagh eltolódás nem térképezhető).

A Hazara szintaxist nagy antiformként értelmezzük, amely meghajlította az MBT és Panjal feltolódásokat egy oligo-miocén molasszmag körül, mely maga is antiformot képez (BOSSART et al. 1988). Modellünkben a nyugati vergenciájú Balakot feltolódás és más, mélyebb vak feltolódások vannak ezen antiform magjában. A szintaxis déli folytatásában a miocénben tapasztalható redők folyamatosan nyomozhatók a Kelet-Potwar régiótól Nyugat-Kásmirig; ezekben a szerkezetekben nem tapasztalható nagyobb törés. E szerkezetek szintén újrarahajlítottak, hogy egy nagyszabású, É–D-i tengelyű antiformot alkossanak. A tágabb terület térképelemzése azt sugallja, hogy É–D-i tengelyű redők bőséggel találhatóak az észak-indiai szegélyen.

Több független adat szól a harántirányú redők létezése mellett: földtani térképek (és űrfotók) elemzése; korábban mért paleomágneses deklináció-irányok, a deformációs ellipsoidok tengelyirányainak szórása mind azt sugallják, hogy az eredeti szerkezetek nagyjából lineáris elrendeződésűek voltak, és később gyűrődtek meg regionális redőkbe, amelyek esetenként a beöblösödő szakaszokat magyarázzák. Ha a korábbi nagy feltolódások lineárisabbak voltak, az ezeken tapasztalható váltó szerkezetek az MBT esetében balos, az MFT esetében hol balos, hol jobbos nyírási komponens jeleznek a nagyméretű feltolódás mellett.

Korábbi (ZEITLER 1985) és most közölt alacsony hőmérsékletű termokronológiai korok egy általános K–Ny-i rövidülési eseményt körvonalaznak 4–5 Ma között az egész észak-indiai szegélyre. Valószínű azonban, hogy a harántirányú redők, dómok keletkezése már az oligocén folyamán megindult (DIPIETRO et al. 2008). Az is világos, hogy a hosszabb É–D-i rövidülési időszakokat csak röviden szakították meg K–Ny-i epizódok.

Több lehetséges magyarázat van a K–Ny-i rövidüléssel szerkezetek kialakulására egy általános É–D-i rövidülési rezsimben. Egyik szerint az egymást meredeken metsző törések elvégződése egy adott zónában (TREOLAR et al. 1992) ellentétes forgásokat generál. Egy másik lehetőség a kulisszas redőződés egy nagy K–Ny-i jobbos vető mentén, szélesebb eltolódási zónában. Valószínűbb azonban, hogy a haránt irányú redőződés az egész indiai lemezt érintette, ezért a legkézenfekvőbb magyarázatot analóg modellek sugallják (REPLUMAZ et al. 2012). Ezek szerint az észak felé haladó Indiai-táblát oldalról egymás felé konvergáló litoszférhatárok szegélyezik. Az észak felé haladáskor a szegélyek mentén kelet–nyugati rövidülés ébred és azokkal párhuzamosan ilyen irányú feltolódások, hegylancok keletkeznek.

Tárgyszavak: Himalája előhegyei; szerkezeti elemzés, oldalsó rámpák, harántirányú redők, kiemelkedés-történet

Abstract

The Himalayan foreland in N Pakistan, dissected by Main Frontal Thrust (MFT) and Main Boundary Thrust (MBT) contains spectacular salients and syntaxes. The lateral (N–S) boundaries between these salients and syntaxes around Kalabagh city and east–south-east of Islamabad were believed to host deep-seated lateral ramps with strike slip movements. However, seismic data in these two sectors suggest that there are N–S trending folds and locally east- or west-vergent thrusts that affect the Palaeozoic–Palaeogene cover of the Indian shield, as well as the Miocene–Pliocene molasse sediments. The proposed lateral ramps cannot be followed on the seismic and nor on maps; instead, both maps and seismic data suggest folding, often on a regional scale of harder Palaeo–Mesozoic–Palaeogene and softer Oligo–Miocene–Plio–Pleistocene cover.

The NE corner of Surghar Range is proposed to be formed of relaying thrust sheets with emergent heads composed of Palaeozoic–Palaeogene and its slightly detached Miocene molasse cover. These relaying imbricates are taken in a southward flexure generated by a major right lateral shear of a wide zone, where transpressive Riedel shears, en echelon anticlines and southwards flexed earlier thrust faults are the main elements (but a single, through-going Kalabagh fault is missing). The generation of mapped N–S trending folds and east-vergent thrusts preceded the formation of the wide shear zone and southwards flexing.

Hazara syntaxis is interpreted as a major antiform that re-folded MBT and Panjal thrust around Oligo–Miocene molasse, itself forming an antiform (BOSSART et al. 1988). In our model we propose that the west-vergent Balakot thrust and deeper blind thrusts are in the core of this antiform. In the southern continuation we propose that folds in Miocene molasse continue from eastern Potwar region to western Kashmir and there appears no major break. These structures are also re-folded in a major antiform with N–S axial trend. Map analysis also suggests that N–S trending folds bending earlier main thrusts are occurring in a wide area south of the Indus–Tsangpo suture.

Several independent geological and geophysical observations including mapping, seismic analysis, earlier measurements of strain axes and of palaeomagnetic declinations suggest that the salients and syntaxes may have been much more linear in the past (although a total linearity is not realistic). It is proposed that the present-day undulating pattern may have been generated by N–S trending folds due to general (and episodic) E–W shortening. If the main fault zones were more linear, the relay pattern along their segments suggests a left lateral shear component along MBT and a mixed, locally left, locally right lateral component along MFT.

Earlier (ZEITLER 1985) and now provided low temperature thermochronological ages strongly suggest a rather general episode of E–W shortening between 4–5 Ma for the whole northern Indian margin. However, there should have been original transversal dome formation as early as Oligocene (DIPIETRO et al. 2008). It is also clear that longer N–S shortening and shorter E–W shortening episodes should alternate eventually in a very short time frame, since earthquake focal mechanisms (LISA & KHWAJA 2004, BURG et al. 2005) suggest the coexistence of E–W compression and NW–SE compression in Potwar.

There are several potential explanations for generating E–W shortening and related structures in a general N–S shortening regime. Possibilities range from fault terminations of thrust faults at high angles in a particular zone (TREOLAR et al. 1992) to en echelon folding along a major right lateral E–W fault zone. However, we speculate that E–W shortening could be much more general, suggesting a mechanism that affects the whole of Indian plate. Possibly the best explanation is given by analogue models (REPLUMAZ et al. 2012) proposing major, slightly convergent confining boundaries. If applied to the northwards advance of India, the northwards converging boundaries generate secondary E–W shortening and east- or west-vergent orogens parallel to these boundaries.

Keywords: Himalayan foothills; structural analysis; lateral ramps; transverse folding, uplift history

Preamble

Frank HORVÁTH was an inspirational person, active at a perfect time for his profession. He lived the best time of Plate tectonics, at least in Hungary, where he actively contributed at the paradigm change. He also worked out and gave a lot of ideas about the tectonics and geophysical structure of the Pannonian Basin, his beloved hunting ground. However, he never stopped at borders, freely swinging between the different Mediterranean chains and between different topics such as palaeomagnetism, lithospheric structure, thermal evolution of the lithosphere or the link between intraplate stresses and topographic features. He has always considered geology-geophysics as an integral science, without subdivisions and he always taught us to apply different branches of this vast kingdom (at least on an educated interpretational level). He always pushed his followers to have correct observations, but also to question the status quo and try to come up with surprising new models better explaining the observations. The topic of the paper was chosen to reflect his multidisciplinary approach in a plate-tectonic context. It also tries to challenge some interpretations that appear quite straightforward at a first approach.

Introduction

The Himalayan chain has two major syntaxes at both eastern and western ends (*Figure 1* insert): the Namche Barwa and Nanga Parbat syntaxes *sensu lato* (e.g. WADIA 1931, GANSSER 1964, BURG & PODLADCHIKOV 1999; BAJOLET et al. 2013). These regions have always attracted attention. However, there are more syntaxes and re-entrants in smaller dimensions especially in the western major syntaxis area. These syntaxes bend around several main fault zones that run along parts or the entire Himalaya (TREOLAR et al. 1992).

The present paper deals with the NE Himalayan syntaxis area in Pakistan (*Figure 1*), however, its aim is not to explain the greater syntaxis (see e.g. BAJOLET et al. 2013; REPLUMAZ et al. 2012), but to give new data on some of the smaller syntaxes–re-entrants in the south. The Surghar and (greater) Hazara syntaxes will be examined in more detail (*Figure 1*). These data indicate the presence of transversal folding, i.e. folds of N–S, rather than E–W axial traces. The idea of E–W shortening and buckling of several structural units is not new; in fact early authors explained the major syntaxial areas by buckling (WADIA 1931, GANSSER 1964, TREOLAR et al. 1992). Numerical modelling has also shown that buck-

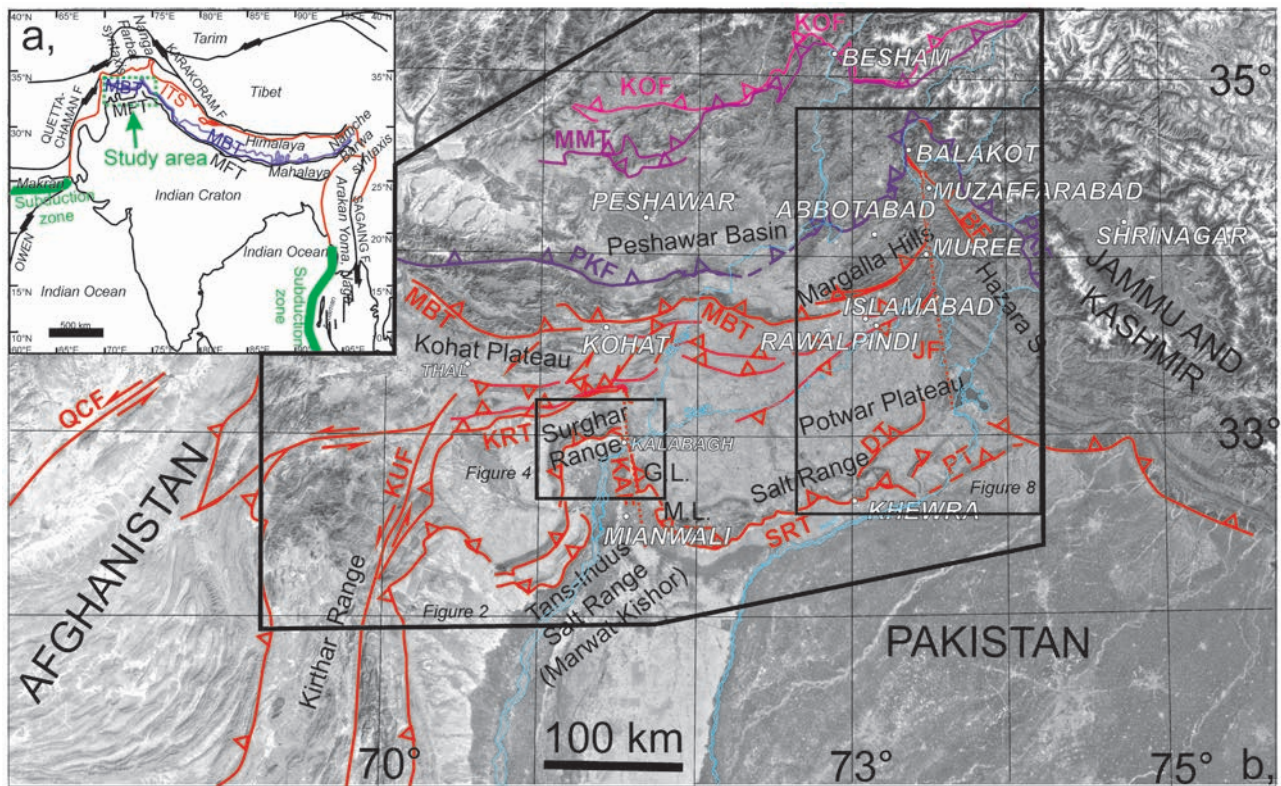


Figure 1. Location map. a) Main structures of the Himalayan region, after BAJOLET et al. (2013), modified. ITS = Indus-Tsangpo Suture; MBT = Main Boundary Thrust, MFT = Main Frontal thrust. b) Satellite image of the study area. Courtesy of Google Earth. Three later figures marked by boxes. G.L. = Gundi Lobe, M.L. = Mussa Khel Lobe, QCF = Quetta-Chaman Fault, KOF = Kohistan Fault, MMT = Main Mantle Thrust, PKF = Panjal-Khairabad Fault, MF = Murree Fault, BF = Balakot Fault; MBT = Main Boundary Thrust, KMF = Khari Murat Fault, KUF = Kurram Fault, KRF = Karak Fault, SRT = Salt Range Thrust, DT = Domeli Thrust, PT = Pabbi Thrust. Stippled fault traces: supposed structures: KAF = Kalabagh Fault, JF = Jhelum Fault

I. ábra. A cikkben tárgyalt terület. a) a Himalája régió főbb szerkezetei, BAJOLET et al. (2013) alapján, módosítva. ITS = Indus-Tsangpo Suture, MBT = Main Boundary Thrust, MFT = Main Frontal Thrust. b) A tágabb terület műholdfotója. Köszönök a Google Earth-nek. A később bemutatott ábrákat keretek jelölik. G.L. = Gundi lebeny, M.L. = Mussa Khel lebeny. QCF = Quetta-Chaman Fault, KOF = Kohistan Fault, MMT = Main Mantle Thrust, PKF = Panjal-Khairabad Fault, MF = Murree Fault, BF = Balakot Fault, MBT = Main Boundary Thrust, KMF = Khari Murat Fault, KUF = Kurram Fault, KRF = Karak Fault, SRT = Salt Range Thrust, DT = Domeli Thrust, PT = Pabbi Thrust. Szaggatott vonallal a feltételezett törések: KAF = Kalabagh Fault, JF = Jhelum Fault

ling on a lithospheric scale is possible and probable (BURG & PODLADCHIKOV 1999). However, mapping in the study area (GEE 1980) suggested long, deep-rooted lateral ramps (MARSHAK 2004) that link more linear E–W segments of major thrusts (Figure 2; dotted faults; e.g. MCDUGALL & KHAN 1990, AHMAD et al. 2010). These are best exemplified by generally accepted maps such as KAZMI & RANA (1982) or NIZAMUDDIN (1997), CRAIG et al. (2018, their Figure 7). The proposed Kalabagh and Jhelum faults of ca N–S trend merit special attention and are in the focus of this paper (Figure 2). It will be shown that these structures do not exist as they are imagined and shown on maps. In contrast, instead of these faults, folds are observed with N–S axial trends. Several competing hypotheses will be discussed to explain the possible reasons of E–W shortening during the obvious N–S shortening of Himalayan orogeny.

Methods

We intend to analyse two sectors: the NE corner of Surghar Range (Figure 2) where Kalabagh Fault was proposed and the eastern part of Potwar Plateau, where the

through-going Jhelum Fault was proposed (Figure 2). We analyse maps and selected seismic lines in these key areas. Additionally, a set of different structural data are collected from literature (BOSSART et al. 1988, BURG et al. 2005) that suggest the existence of N–S axial trend folds and E–W shortening. Results of our low temperature thermochronologic study (apatite fission track and [U–Th]/He) in the Potwar Plateau are also given to offer some timing constraints for the deformation.

Regional geological framework

Himalaya is structurally dissected into several major units. The limiting shear zones run along the entire chain. There are reportedly two suture zones: the Shyok and Indus sutures (the latter also named Main Mantle Thrust) that separate Eurasian, Kohistan island arc and Indian origin rocks (TREOLAR et al. 1992). South of the Main Mantle Thrust (MMT; Figure 2) we can find different parts of the Indian continent that is subthrust beneath the northern island arcs, microcontinents and finally the Eurasian plate (e.g. MATTAUER 1983).

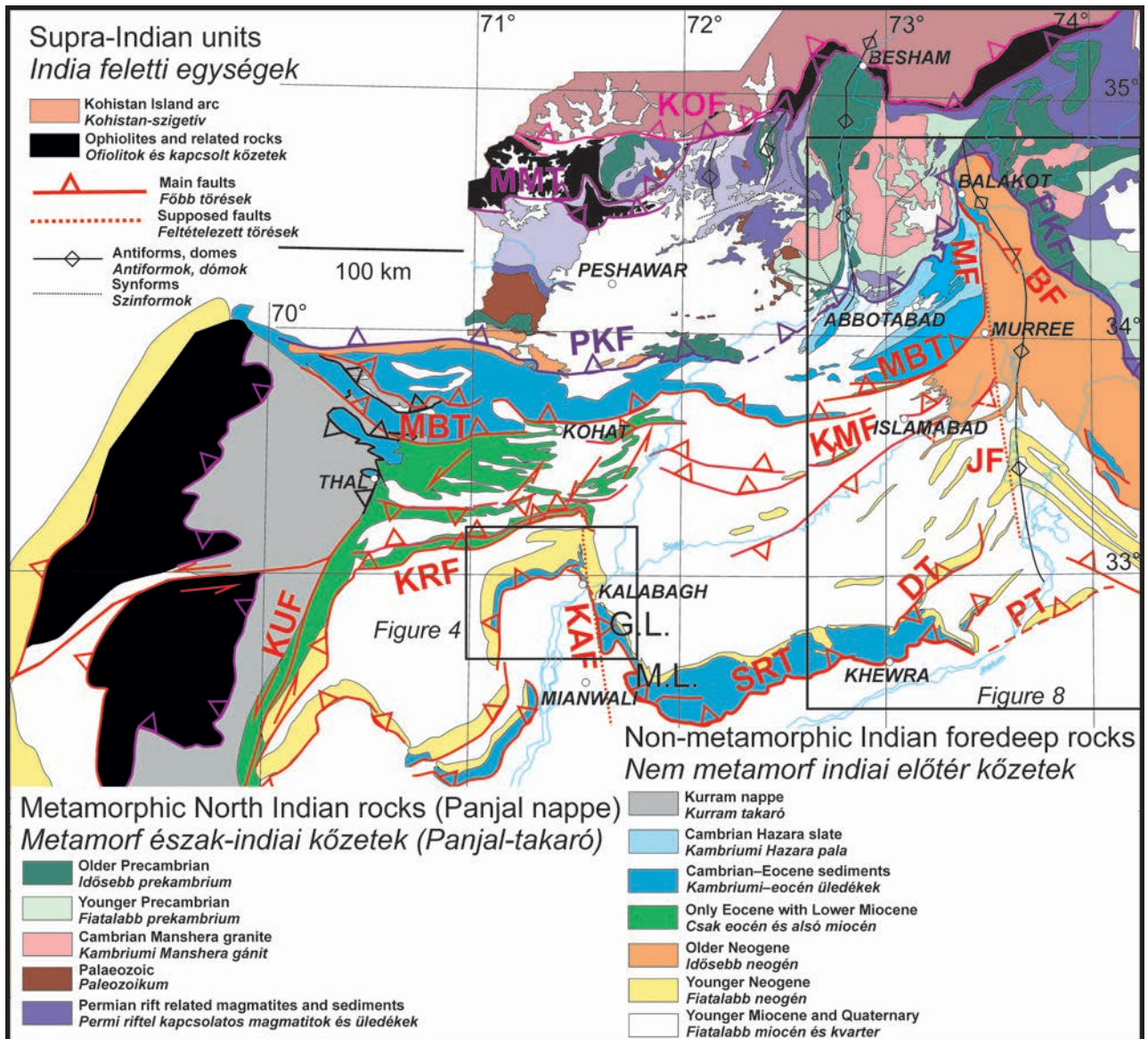


Figure 2. Simplified geologic map of the study area. Constructed after: CALKINS & OFFIELD (1974), GEE (1980), DiPIETRO et al. (2008), GHAZI et al. (2014), JADOON et al. (2015), GHANI et al. (2018). Kalabagh and Jhelum faults traced after KAZMI & RANA (1982). Later figures marked by boxes. G.L. = Gundi Lobe, M.L. = Mussa Khel Lobe. KOF = Kohistan Fault, MMT = Main Mantle Thrust, PKF = Panjal-Khairabad Fault, MF = Murree Fault, BF = Balakot Fault, MBT = Main Boundary Thrust, KMF = Khari Murat Fault, KUF = Kurram Fault, KRF = Karak Fault, SRT = Salt Range Thrust, DT = Domeli Thrust, PT = Pabbi Thrust. Stippled fault traces: supposed structures: KAF = Kalabagh Fault, JF = Jhelum Fault

2. ábra. A terület egyszerűsített földtani térképe, CALKINS & OFFIELD (1974), GEE (1980), DiPIETRO et al. (2008), GHAZI et al. (2014), JADOON et al. (2015), GHANI et al. (2018) nyomán szerkesztve. A Kalabagh és Jhelum töréseket KAZMI & RANA (1982) nyomán rajzoltuk. G.L. = Gundi lebeny, M.L. = Mussa Khel lebeny. KOF = Kohistan Fault, MMT = Main Mantle Thrust, PKF = Panjal-Khairabad Fault, MF = Murree Fault, BF = Balakot Fault, MBT = Main Boundary Thrust, KMF = Khari Murat Fault, KUF = Kurram Fault, KRF = Karak Fault, SRT = Salt Range Thrust, DT = Domeli Thrust, PT = Pabbi Thrust. Stippled fault traces: supposed structures: KAF = Kalabagh Fault, JF = Jhelum Fault

In Pakistan, the most important boundaries are the following (Figure 2). The Indus–Tsangpo (MMT) suture indicates the suture zone of the Indian continent-origin rocks and the Kohistan Island arc (TREOLAR et al. 1992); however, a northern Kohistan Fault was also separated as an important younger boundary (DiPIETRO et al. 2008). The Panjal–Khairabad (or Tarbela) thrust separates a series of northern thrust sheets, composed of older and younger Precambrian crystalline basement, Cambrian granitic intrusion; erosional remains of a Palaeozoic sedimentary sequence; Permian alkali magmatites (both intrusive and effusive) and an older

Mesozoic assemblage related to rifting (Figure 2). These rocks all suffered varying degrees of metamorphism, from low grade in the south to high grade in the north (TREOLAR et al. 1992), whereas south of the Panjal thrust rocks are non- to anchimetamorphic (BOSSART et al. 1988). In maps east of Abbotabad, Panjal thrust continues in the north of the Hazara syntaxis above the ‘Panjal imbricates’ of BOSSART et al. (1988), TREOLAR et al. (1992). Further south of the metamorphic Precambrian–Mesozoic succession comes a unit bordered on the south by the Main Boundary Thrust (Figure 2, MBT; TREOLAR et al. 1992, BURG et al. 2005). This fault

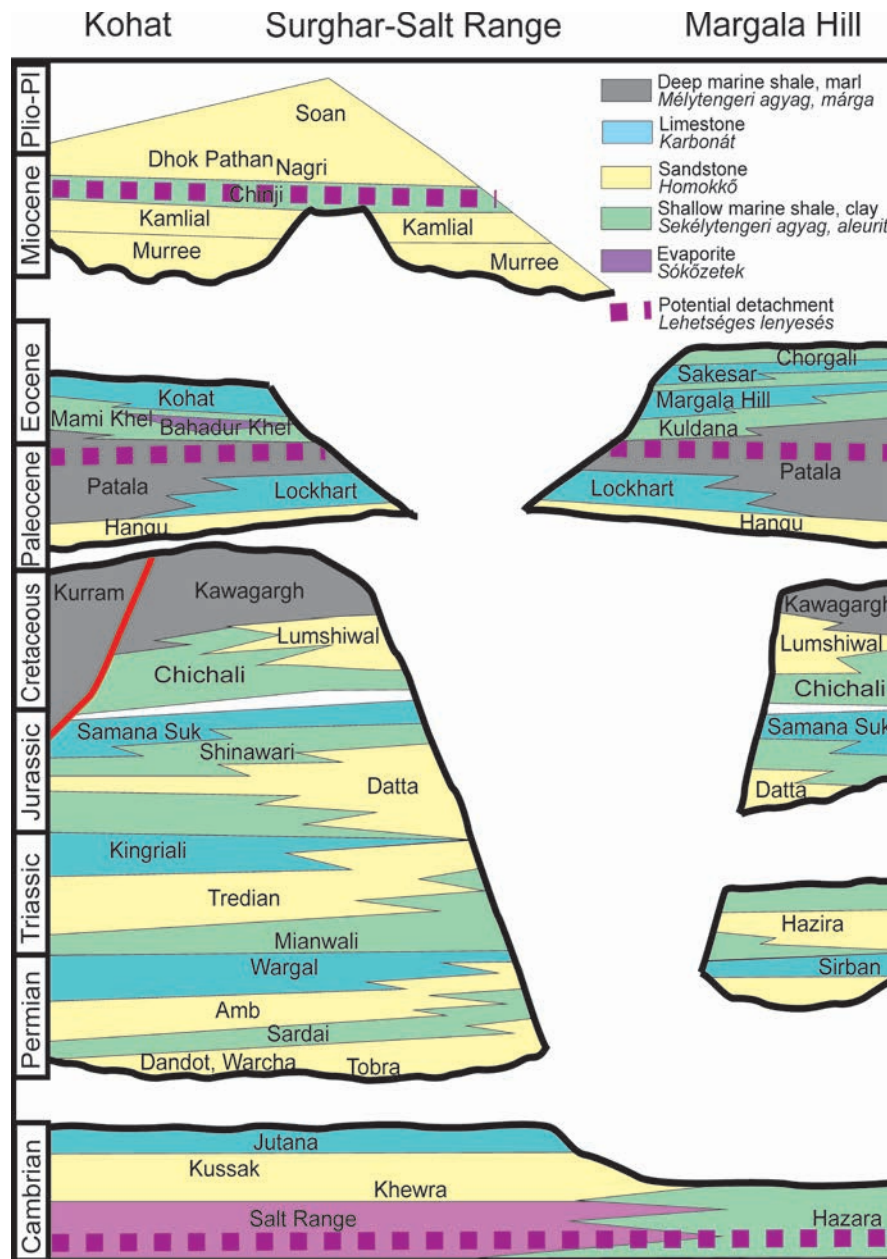


Figure 3. Stratigraphic chart of the Pakistani Himalaya foothills area. Modified after GRÉLAUD et al. 2002, BURG et al. 2005, GHANI et al. 2018

3. ábra. A pakisztáni Himalája előtér rétegtani táblája. GRÉLAUD et al. 2002, BURG et al. 2005, GHANI et al. 2018 nyomán, módosítva

runs mostly along a sharp topographic boundary, opposing non-metamorphic Mesozoic–Palaeogene rocks in hilly terrain to mostly Mio–Pliocene molasse sediments in the southern lowlands, plateaus. However, there is no major difference in the subsurface stratigraphic composition of the southern lowlands and the northern hilly part, on either side of MBT. In other words, MBT is rather a sharp topographic boundary, just one of the many thrust faults that affect the non-metamorphic region. In the east, at the Margala Hills (Figure 1) the northern unit is composed of stacked imbricates and is thrust over the North Potwar Deformed Zone (NPDZ), yet another thrust imbricate zone (TREOLAR et al.

1992, JASWAL et al. 1997, JADOON et al. 1997). In this region, the amount of overthrust along MBT can be quite significant (see TREOLAR et al. 1992 and later). In the west (Figure 2) the mainly Mesozoic rocks above MBT are thrust over the Kohat Plateau, where mostly Eocene rocks with their Miocene molasse cover are exposed (VETRUM et al. 2011). However, the Mesozoic is preserved beneath the Palaeogene. In the westernmost part a nappe, Kurram unit, is found above the Mesozoic–Palaeogene (Figures 2, 3). This is composed of deep marine, mostly turbiditic sediments.

Even further south the Main Frontal Thrust (MFT) indicates a zone of southernmost thrusts which put Late

Precambrian–Eocene sediments against their southern Plio–Pleistocene foredeep (*Figure 2*; YEATS et al. 1984, GRÉLAUD et al. 2002, GHANI et al. 2018). A continuous mountain chain (*Figure 1*) composed of the Trans-Indus Salt Range, the Surghar Range and the Salt Range mark the southernmost edge of large thrusts. The Kohat and Potwar Plateaus provide the hinterland to this mountain chain and travel on their back towards the south. The trace of MFT is curvilinear, forming several syntaxes. The fault can be followed from the Kirthar Range until the eastern termination east of Khewra (*Figure 1*). The southernmost foreland seems only slightly deformed and covered by very young (Pleistocene) sediments (YEATS et al. 1984, MEIGS et al. 1995, QAYYUM et al. 2015).

General stratigraphy

South of the Panjal–Khairabad Thrust the stratigraphy of the Indian shield is rather uniform (GEE 1980). The first sediments on crystalline basement are a Late Proterozoic–earliest Cambrian rock salt formation (Salt Range formation; *Figure 3*) hosting one of the earth’s oldest salt mines at Khewra and at the origin of the worldwide sold ‘Himalayan salt’. This ductile rock is found at the basis of the southernmost thrusts of the Salt Ranges and provides a perfect detachment zone in the Potwar Plateau as well. It might be present in other parts (e.g. beneath the Surghar Range and Kohat Plateau) but not proven yet. The salt formation is overlain by a sequence of Cambrian continental–shallow marine formations including sandstones and dolostones. The Cambrian formations can be 500–100 m thick (thickness being modified by salt tectonics; GHAZI et al. 2014).

After a long break in sedimentation and an unconformity, Permian glacial sandstones, tillites and conglomerates, then carbonates are deposited, to be followed by an apparently concordant sequence of Triassic–Jurassic–Cretaceous rocks (GHAZI et al. 2014). The individual formations may follow local hiatuses. However, a repetitive sequence of sandstones, marls, shallow water carbonates is regularly observed as controlled by eustatic sea level oscillations at the northern passive margin of the Indian plate.

A major unconformity with locally deep cutting erosion is observed in the Palaeocene. This unconformity probably indicates the first collision episode of the Indian margin with the Kohistan arc (TREOLAR et al. 1992). It erodes sediments towards the SE, so the Mesozoic and partly the Permian are missing in SE Potwar (GHAZI et al. 2014). The unconformity is overlain by sandstone, limestone and deep marine shale-marl deposited in a foredeep basin. The basin topography is gradually filled up by Eocene shale, clay, evaporite and several levels of shallow water limestone. The most prominent is the Kohat Limestone that forms smaller mountains and ridges in the Kohat Plateau (VETRUM et al. 2011).

The total thickness of Permian to Palaeogene is 1 500–2 000 m in Kohat Plateau (VETRUM et al. 2011), while it is reduced to 500–200 m in the Potwar Plateau and Margala

Hills. Locally, Palaeogene may thicken in Kohat because of tectonic reasons (GHANI et al. 2018).

Again a major break and an unconformity is observed at the top of Eocene (*Figure 3*). (Oligocene)–Miocene–Pliocene–Pleistocene continental sediments are deposited locally in huge thickness (in excess of 6–7 km) on top of the older formations (GHAZI et al. 2014). Most of these sandstones–shales–conglomerates have fluvial origin and gradually fill up the subsiding Himalayan foredeep. The formations are diachronous and show strong lateral thickness variations (GRÉLAUD et al. 2002, GHAZI et al. 2014). Dating was mostly done on the basis of palaeomagnetic zonation, calibrated by rare radiometric ages of tuff horizons and even rarer fossil record (JOHNSON et al. 1982, 1986; MEIGS et al. 1995; GRÉLAUD et al. 2002); Eocene oldest ages for this molasse (BOSSART & OTTINGER 1989) have been revised to be at least Oligocene or younger (NAJMAN et al. 2002). The Murree Formation, the oldest member of the molasse is generally assumed to range from 22 Ma to 18 Ma (e.g. JOHNSON et al. 1982, MEIGS et al. 1995, GRÉLAUD et al. 2002); this formation occupies most of the Hazara syntaxis core area as well as the mountains immediately SE of the Margala Hills (*Figure 2*). It is also present in limited thickness in the Kohat Plateau. The overlying Kamli Sandstones range until 14–13 Ma (JOHNSON et al. 1982, GRÉLAUD et al. 2002). This formation is exposed in the cores of folds north of Soan syncline in Potwar and on fold limbs in Kohat Plateau (*Figure 2*). The Chinji red shale–clay is discordantly overriding older molasse as well as eroded older sediments. This is the first Miocene cover on the Surghar and the Salt Ranges (MEIGS et al. 1995, GHANI et al. 2018). Its age spans to 10.8–10 Ma (JOHNSON et al. 1982, GRÉLAUD et al. 2002). The overlying Nagri and Dhok Pathan Formations span until 8.8–7.9 Ma and 5.7–5.1 (JOHNSON et al. 1982, GRÉLAUD et al. 2002). The youngest Soan Formation and local conglomerates, silts are Late Pliocene–Pleistocene in age.

Eastern Surghar Range

Surghar Range (*Figures 1, 2, 4*) is an exposure of Permian–Eocene rocks, topped by the Miocene molasse, that are all overthrust to the south on top of Plio–Pleistocene molasse (underlain by the same stratigraphy as the Hanging-wall; DANILCHIK & SHAH 1987, GHANI et al. 2018). The range is composed of three different segments: the Makarwal segment of N–S, the Surghar segment of E–W and the Western Salt Range segment again of N–S orientation (*Figure 4*). The latter is composed of individual lobes: the Gundi and Mussa Khel Lobes (MCDUGALL & KHAN 1990, GHANI et al. 2018; *Figure 1*). Along the range Jurassic–Eocene sediments are exposed in the higher mountain part. They are overridden by Late Miocene Chinji and Nagri Formations; younger terms of the molasse are also present further north and in the east, i.e. on the western Potwar Plateau (DANILCHIK & SHAH 1987). Cambrian–Palaeozoic formations are only exposed in the Western Salt Range,

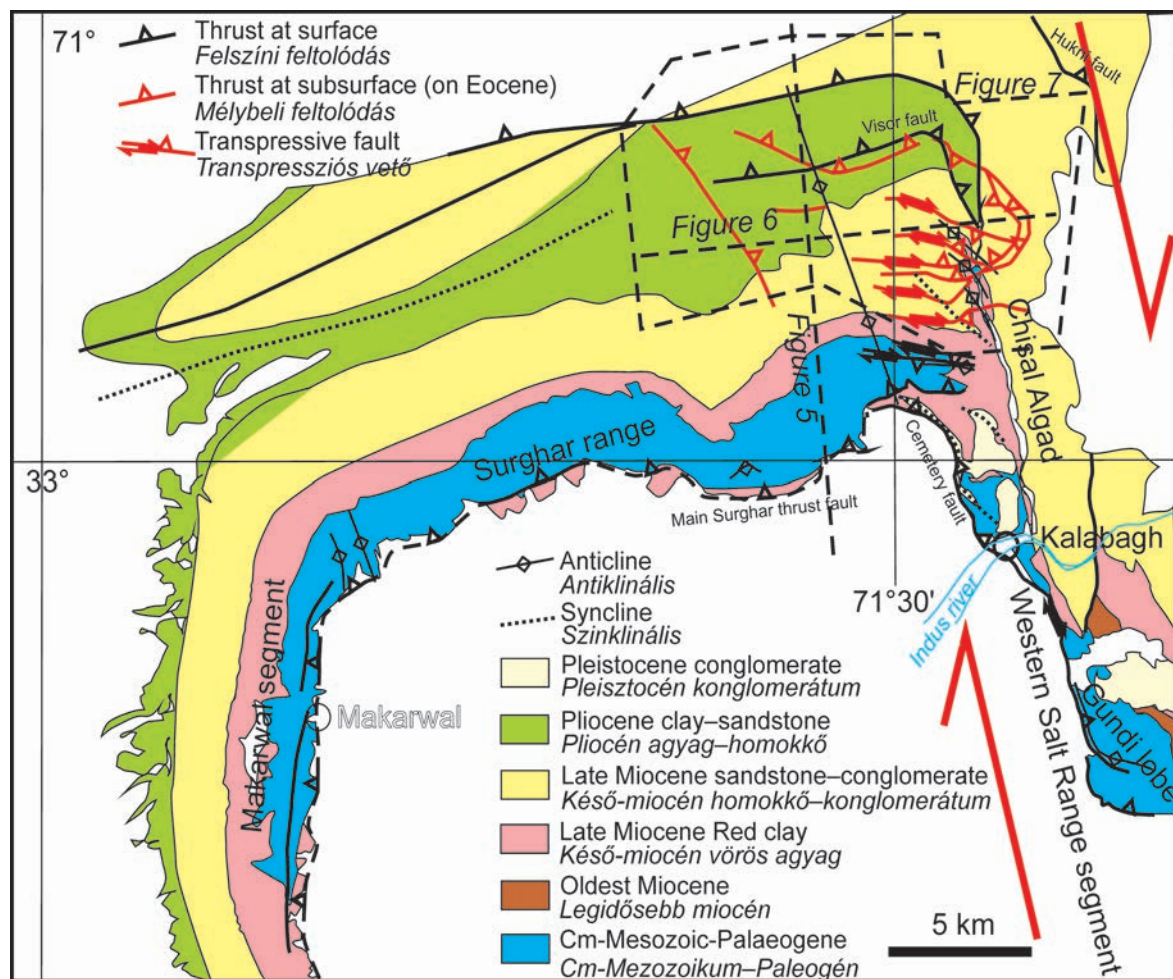


Figure 4. Simplified geological map of the Surghar Range, Western Salt Range area, after GEE (1980), DANILCHIK & SHAH (1987), own observations. locations of later figures in stippled lines

4. ábra. A Surghar Range - Western Salt Range terület egyszerűsített földtani térképe, GEE (1980), DANILCHIK & SHAH (1987), nyomán, saját megfigyelésekkel módosítva. Későbbi ábrák helyei szaggatottal jelölve

while Permian–Triassic is exposed locally at the NW corner, between the Makarwal and Surghar segments. In other places the deepest exposed stratigraphic term is Jurassic (GEE 1980, DANILCHIK & SHAH 1987). According to own observations in both the Makarwal and the Surghar segments, the formations are folded into tight, eastward and southward facing folds with Jurassic cores. The inward limbs are subvertical to overturned; even Eocene, eventually also Late Miocene Chinji Formation take part in this folding. Thrusts are either not exposed, or not evident on the surface; only a small portion at the central southern part of Surghar segment may expose the main thrust. In most of the range the main thrust (see later) remains blind and buried close to the surface (Figure 4).

In the eastern termination of the Surghar segment there are two relaying ranges of Palaeozoic–Eocene succession locally underlain by the Cambrian Salt Range formation. The northern one terminates by an anticline plunging to the east; cut in the north by a steep E–W fault. The southern exposure, near Kalabagh has a main NW–SE orientation and is overlain by Miocene molasse. However, both are

eroded and overlain by a Pleistocene conglomerate (GEE 1980, YEATS et al. 1984, MCDUGALL & KHAN 1990, GHANI et al. 2018). All these structures are flanked from the SW by the ‘Cemetery fault’ (Figure 4; same authors). A smaller set of exposures is found in the continuation of this rock body south of Indus river, then terminates in a lenticular shape.

Further south another lenticular shape body is found in the direct continuation: the Gundi Lobe (Figure 4). While the Kalabagh lens is very tightly and complexly folded, the Gundi Lobe exhibits a tight, but simple anticline with a southern steep limb. In most maps (GEE 1980, DANILCHIK & SHAH 1987, MCDUGALL & KHAN 1990, GHANI et al. 2018) this is underlain by a SW-facing thrust. Yet another exposure of Palaeogene strata is found in an imbricate directly beneath and south of the former thrust-fold structure.

In simple terms all the structures and formations seem to curve southwards, towards the Western Salt Range segment. The change in orientation occurs near the city of Kalabagh, at a spectacular break-through of the Indus river. Longer fault segments on the western side of the Western Salt Range segment run NNW–SSE. The fault between the

Kalabagh and Gundi lenses apparently continues northwards in a topographic low, called Chisal Algad (*Figure 4*), along which several small exposures of Salt Range salt plugs occur (GEE 1980, YEATS et al. 1984, MCDUGALL & KHAN 1990, GHANI et al. 2018). All authors suggest that the whole N–S oriented zone, from Chisal Algad to the Western Salt Range segment was a major Pleistocene right lateral shear zone (GEE 1980, KAZMI & RANA 1982, YEATS et al. 1984, MCDUGALL & KHAN 1990, AHMAD et al. 2010, GHAZI et al. 2014 and their *Figure 11*, GHANI et al. 2018, their *Figures 3, 12*; CRAIG et al. 2018, their *Figure 5*). According to this interpretation a lateral ramp was generated along Chisal Algad and its due south continuation that right laterally offset the Kalabagh and Gundi Lenses with respect to each other. The so defined Kalabagh Fault accounts for more than ten km right lateral offset (varying according to authors). Most authors (e.g. MCDUGALL & KHAN 1990, AHMAD et al. 2010) continue the Cemetery Fault northwards into a ‘Surghar Fault’ (not displayed on *Figure 4*) that runs until the eastern tip of the northern Cambrian–Eocene exposure. According to them the Kalabagh lens was again right-laterally offset along the ‘Surghar Fault’ from the northern exposures.

MCDUGALL & KHAN (1990) described field exposures in detail, yet they did not find any exposed trace of a major right lateral fault. On the other hand, they did find several east-dipping thrusts offsetting even Quaternary conglomerates and steeply dipping Pliocene sediments.

Own observations

Petroleum exploration in the region, and in the very corner in question produced helpful seismic sections, 3D cubes in a structurally very interesting area. In the following a N–S oriented, and an E–W oriented seismic section is shown, together with a time slice of a 3D cube.

The N–S oriented section (*Figure 5*) shows the Surghar Range hangingwall as a tabular slab with minor internal deformation, that is pushed onto its young foreland. There may be smaller local thrusts within the older formations of that foreland, close to the basal thrust of Surghar. However, due to a possible velocity-pull-up effect, the amount of imbrication and local uplift within the foothill zone is hard to estimate. The slab-like behaviour of the hangingwall geometry suggests a ductile detachment, i.e. possible presence of Salt Range formation (in spite of the fact, that it is not exposed anywhere in Surghar–Makarwal segments). The major thrust fault propagates upwards, but based on mapping it is not exposed; therefore, it should run blind along a shallow detachment within the Plio–Pleistocene. The tight, southwards overturned folds seen in surface sections are not imaged by seismic because of technical limitations; they are drawn on the figure based on surface observations. There may be smaller thrusts both towards the south and towards the north on the back-limb of the thrust. Some of these are quite steep and form WNW–ESE linear

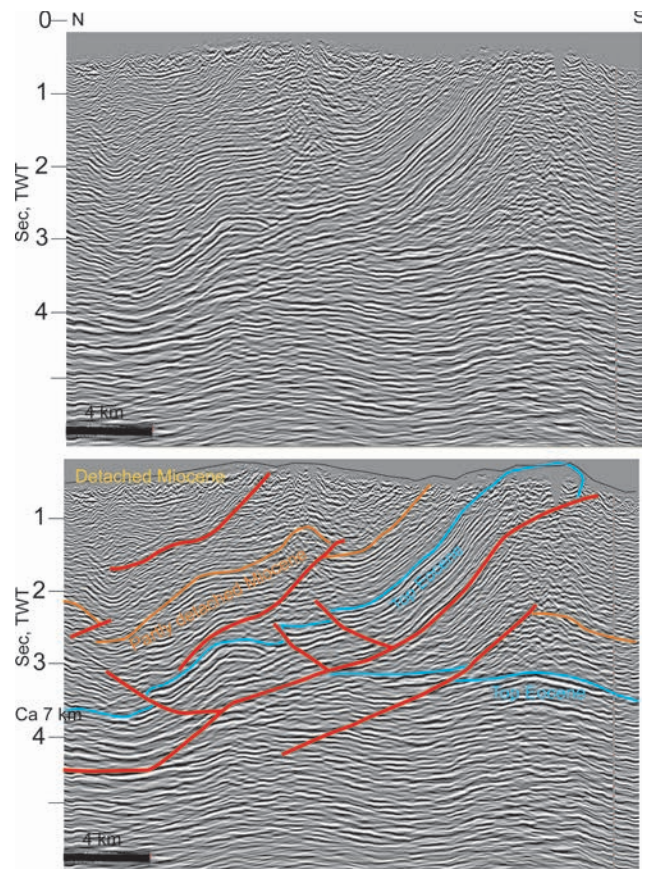


Figure 5. N–S 2D seismic section across Surghar Range; uninterpreted and interpreted time sections. TWT = Two-way travel time. For location see *Figure 4*. Red indicates interpreted faults

5. ábra. É–D-i 2D szeizmikus időszelvény a Surghar-hegyláncban keresztül, értelmezetlen és értelmezett változat. TWT = kétutas futási idő. A szelvény helyzete a 4. ábrán. A vörös vonalak feltolódásokat jelölnek

segments with varying offsets in the eastern part of the 3D area (*Figure 4*; such faults are not seen on *Figure 5* since they are found east of the section trace). Because of their steep dips it is suggested that these are transpressional faults. Right lateral offsets (shown on *Figure 4*) are just indicative because true offsets other than thrusts could not be revealed.

There are several folds, associated thrusts that can be interpreted within the Miocene succession (*Figure 5*). It seems that there are at least two detachment horizons within Miocene: one at its base (possibly Chinji Fm); another higher in the section (possibly higher in Nagri Fm see *Figure 3*). The surface structural expression of faults and thrusts might be entirely detached from the Cambrian–Eocene level structures (*Figure 5*). This is also suggested by the map (*Figure 4*), where the surface structures (in black) do not correspond at all to the ones mapped on the top Eocene of the backlimb of the Surghar slab (in red).

The E–W section (*Figure 6*; taken from the 3D cube) shows surprising features. First, it displays a regional fold with roughly N–S axial trace just north of the eastern lobe of Surghar segment (*Figure 4*). This anticline can be followed not only in pre-Eocene but also in Miocene formations as

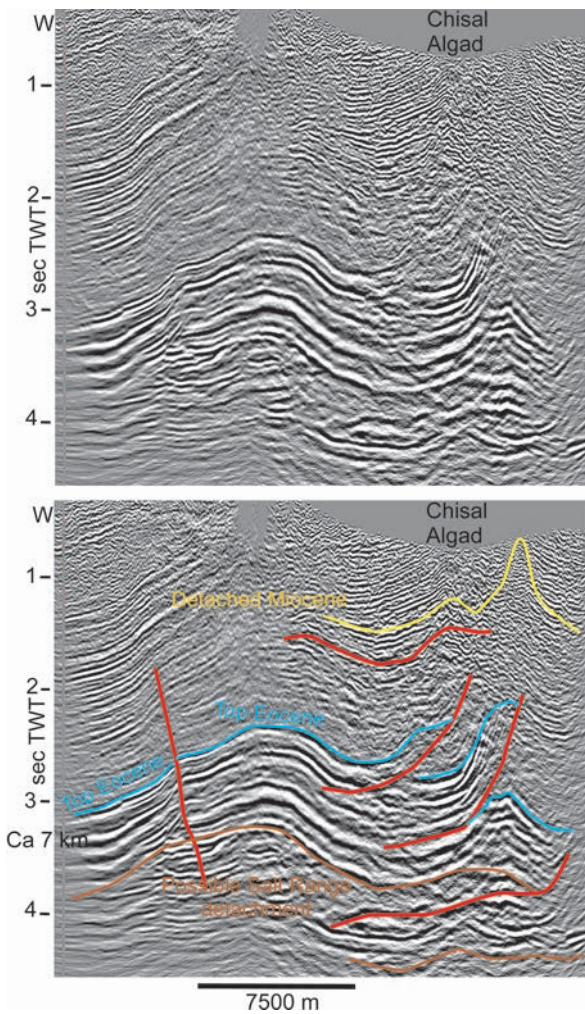


Figure 6. W–E 3D seismic section across northern limb of Surghar Range; uninterpreted and interpreted time sections. For location see Figure 4. Red indicates interpreted faults

6. ábra. Ny–K-i 3D szeizmikus időszelvény a Surghar-hegylánc északi lejtőjén. A szelvény helyzete a 4. ábrán. A vörös vonalak feltolódásokat jelölnek

well (Figure 6), therefore it should be a young feature. The anticline is also clearly seen by a minimal recess within the eastern termination of Surghar segment (Figure 4). All structures, main Surghar Fault and Cemetery Thrust included are gently bent by this fold of NNE–SSW axial trace.

The eastern limb of this anticline (Figure 6) shows two imbricates with eastern vergency; Eocene and older rocks are clearly thrust on top of each other. Moreover, in the easternmost part a deeper anticline within Eocene and older rocks are also seen. This deeper structure is clearly along the strike of the surface Western Salt Range segment. To be noted is the strong discrepancy between surface structures (tight anticlines in Chisal Algard region) and those in the underlying Cambrian–Eocene succession. At least one detachment in Miocene can be inferred (Figure 6). There is also no direct link between the surface and deep structures; presence of salt plugs within Miocene in Chisal Algard should be the result of salt extrusion and rise along a combination of faults in the lower and detached Miocene sections.

On the western limb of the anticline a steep thrust fault

E with NNW–SSE orientation is seen (Figure 6). This fault has varying offsets and since it does not interrupt surface exposures (Figure 4), it is inferred to die out towards the south. However, this fault cannot be mistaken with the earlier proposed Kalabagh Fault.

The most surprising in the E–W seismic section (Figure 6) is the lack of any interruption, break, change in seismic reflection character along the main valley, Chisal Algard, the proposed trace of the regional, deep seated Kalabagh Fault. Instead, Miocene reflectors above the two imbricates clearly suggest a tight anticline made of young rocks (Figure 6). These tight anticlines are also interpreted on the map (Figure 4) as a set of en echelon folds with NNW–SSE orientation.

E The time slice (Figure 7) shows the above described structural features in a map-view section. One can clearly identify the major, regional anticline (with a local imbricate structure in the north, see also Figure 4) and the two east-ward vergent imbricates (Figure 7) that have both a curvilinear, northwards flexed thrust surface. These eastwards thrust faults have a different map view (Figure 4) because the map

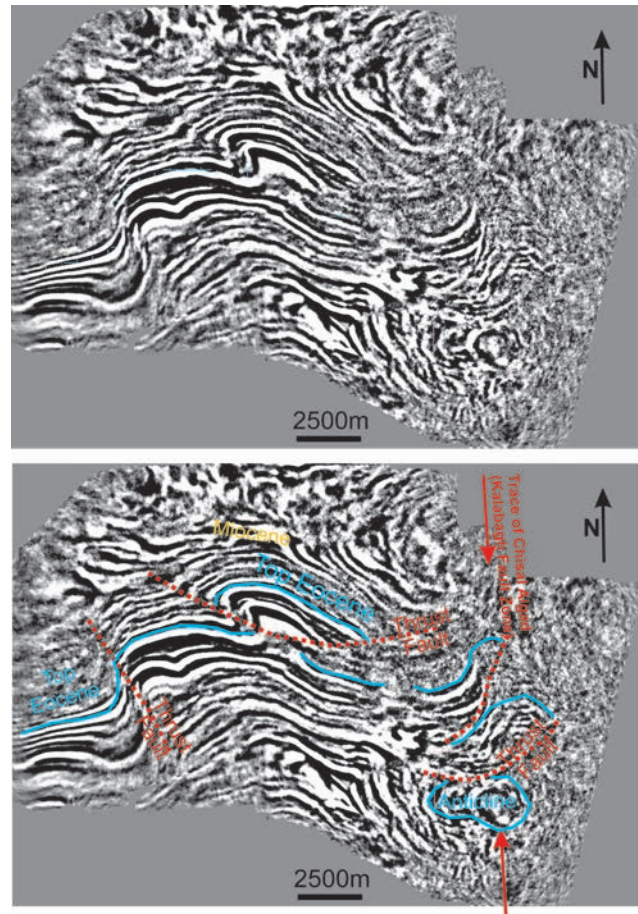


Figure 7. Time slice at 2.9 seconds from 3D cube, uninterpreted and interpreted versions. Location on Figure 4. Note the absence of any deep-seated interruption, break along the trace of Chisal Algard valley, the supposed trace of Kalabagh Fault (red arrows). Red stippled lines indicate interpreted thrusts

7. ábra. 2,9 secundumos időszelvény a 3D tömbből, értelmezetlen és értelmezett változat. A szeizmikus felületen a vörös nyíllal jelölt csapásban (Chisal Algard-völgy) semmilyen mélyre hatoló lineáris, törésszerű elem (Kalabagh törés) nem látható. A szaggatott vörös vonalak az értelmezett feltolódásokat jelölik

shows the fault cut-off at Top Eocene level and not at horizontal (i.e. iso-time) as the time slice. A smaller elliptical outline of the fold located at the deeper eastern part of *Figure 6* is also seen to the south of the top-eastward imbricates. We can also see in the south-easternmost area, that the Surghar Range exposed part will curve southwards as the surface geology (*Figure 4*) suggests.

Again, the most surprising is that there is no apparent major boundary, break, offset along the proposed trace of the Kalabagh Fault that should be a deep-seated, regional lateral ramp (GEE 1980, KAZMI & RANA 1982, YEATS et al. 1984, McDUGALL & KHAN 1990, AHMAD et al. 2010, GHANI et al. 2018).

A closer look at the surface geology of the area (*Figure 4*) suggests that some deep structures are not detached from their Miocene cover. In the NW corner of Surghar Range, between the Makarwal and Surghar segments the Palaeozoic–Eocene rocks, together with their direct Miocene cover both curve southwards towards Makarwal. It is interesting to note that in the internal, southern part of the curvature the Permian–Triassic–Jurassic strata are taken into N–S axial trace folds (*Figure 4*; DANILCHIK & SHAH 1987). In the south-eastern portion between the Surghar and Western Salt Range segments Cambrian and its Miocene cover also turn southwards together. However, in the NE part of the map, along Chisal Algad, one can observe that red Late Miocene clay (Chinji Fm), the oldest term of Miocene cover, turns northwards across a syncline and forms a series of tight anticlinal cores (*Figure 4*). In the very heart of these, two tiny exposures of Cambrian salt occur. These tight anticlines are probably detached from the eastwards facing Eocene-older imbricates at depth (*Figures 4, 6*). The eastern side of the valley consists of Late Miocene–Pliocene formations in the cover of the red clays. Although there might be minor offset along local faults, no major, regional and pluri-kilometric fault is needed to explain the geology. In short, the regional, deep-seated Kalabagh Fault is not needed.

In the north, north of Chisal Algad the map (*Figure 4*) shows a series of curvilinear thrust faults that repeat parts of the Miocene section (Visor Fault system; DANILCHIK & SHAH 1987) or that cut up from the Eocene and die out in Miocene (Hukni Fault; GHANI et al. 2018). The eastern termination of both faults curve southwards. Since the southwards curvature is apparently coherent with a southwards advancing Salt Range frontal thrust with respect to a trailing Surghar frontal thrust, most authors (GEE 1980, KAZMI & RANA 1982, YEATS et al. 1984, McDUGALL & KHAN 1990, AHMAD et al. 2010, GHAZI et al. 2014, GHANI et al. 2018) suggest that their proposed Kalabagh Fault should run along the Chisal Algad and be linked to the southwards flexed tip of Visor and/or Hukni (or only Visor) thrust faults. On the seismic (mostly on E–W lines, but not on *Figure 6*) the Visor fault can be indeed seen as a geometric unconformity within the Miocene. This is a relatively flat thrust that cannot be directly rooted into any mapped structure in the Cambrian–Eocene sequences. Eventually the limits of 3D volume do not enable to further detail that question.

Summarising the observations in this sector (*Figure 4*),

there are obvious indications of major N–S shortening, like the basal thrust along the Surghar segment. However, beside this (general) southwards structural transport there are multiple structures formed by E–W (ENE–WSW) shortening. In short, the local structures suggest much more folding of an originally more linear or slightly undulating orogen, than major right lateral or left lateral fault offsets along the N–S segments. Near Kalabagh and in particular along Chisal Algad, no regional, deep- or even shallow-seated fault could be observed and indeed, it is not needed to adequately explain the surface and deeper geological structures. On the eastern limb of the N–S trending fold a localised series of steep transpressive faults with E–W orientation are found in a wider zone with N–S orientation, along the Chisal Algad. A potential explanation for this zone is given in the Discussions.

Eastern end of Potwar Plateau and of Margala Hills

The region consists of four quite distinct geological areas (*Figure 8*): 1) the Margala Hills (BURG et al. 2005), limited to the south by the Main Boundary Thrust (MBT); 2) the North Potwar Deformed Zone (NPDZ; JASWAL et al. 1997; JADOON et al. 1997, 1999) south of MBT and north of the Soan syncline; 3) the Salt Range and its northwards limb, comprised between the Soan syncline and the Salt Range boundary thrust (GRÉLAUD et al. 2002), 4) finally the Hazara syntaxis, which is found to the east and north of the former areas (BOSSART et al. 1988).

1) Margala Hills is a range gradually elevated from west to east up to 3 km asl (*Figure 1*). It is composed of Jurassic–Eocene sediments, underlain by Late Proterozoic–Early Cambrian shales, the lateral equivalents of Salt Range formation (e.g. BURG et al. 2005). The Eocene succession terminates by the red Kuldana shales that may form a detachment. The Palaeocene Patala Shale may form an additional detachment (*Figure 3*). The sedimentary contact of Palaeozoic and Jurassic is preserved in a northern unit, which has the same characteristics as the Margala Hills s.str, but which are found north of the Hazara–Natia Gali Thrust (*Figures 8, 9*; BURG et al. 2005). For some (e.g. TREOLAR et al. 1992) the Margala Hills are composed of stacked imbricates; for some others (e.g. BURG et al. 2005) one single unit builds up the area.

The exposed rocks are very intensely deformed; this is expressed as map scale folds and thrusts of different size (LATIF 1968) to outcrop scale folds of different orientations. BURG et al. (2005) give at least three different axial orientation for these folds: ENE–WSW; NW–SE and N–S. These measurements coincide with our observations (*Figure 9*). Faults are rarely exposed, nevertheless BURG et al. (2005) were able to reconstruct palaeo-tensors for 16 of their sites (the others did not satisfy their calculation criteria). Coinciding with fold directions, the main sigma1 orientations were: NNW–SSE to NE–SW and E–W; with several strike slip type stress tensors. These authors emphasised the importance of transpression and imagined the Margala Hills as

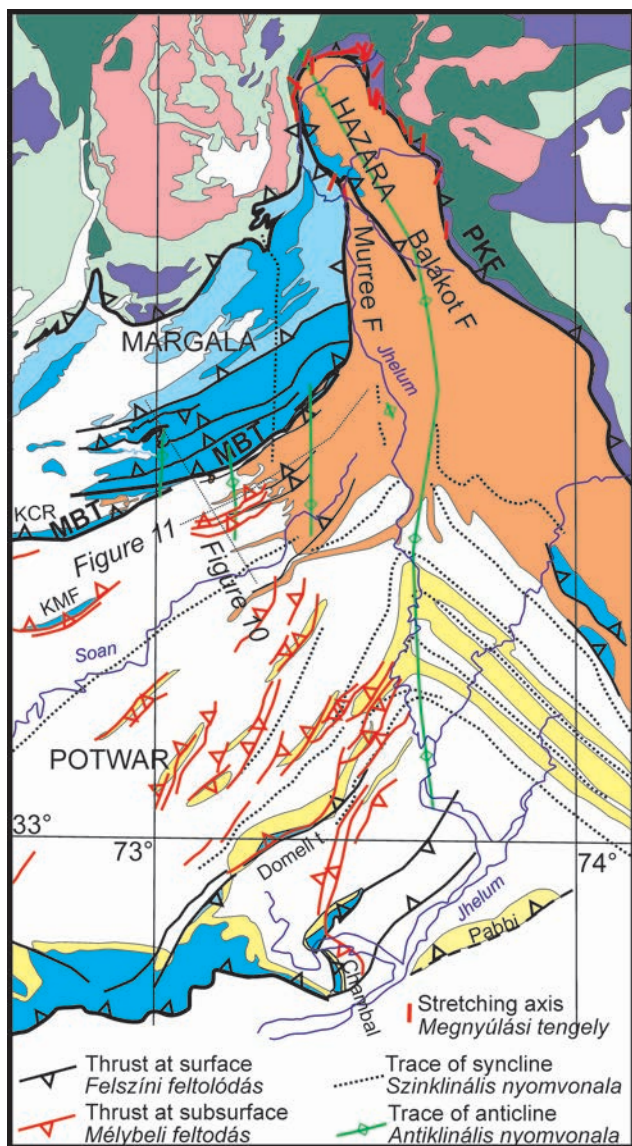


Figure 8. Blow-up geological map of the Margala Hills, Potwar, Hazara and Salt Range area. simplified and modified after CALKINS & OFFIELD (1974), BOSSART et al. (1988), BURG et al. (2005), QAYYUM et al. (2015) and GHAZI et al. (2014), incorporating a manuscript map of S. AHMAD

PKF = Panjal-Khairabad Fault; MBT = Main Boundary Thrust; KMF = Khari Murat Fault; KCR = Kala Chitta Range. Later figures marked as thin stippled lines. Red sticks around the Hazara syntaxis indicate long axes of strain ellipsoids measured by BOSSART et al. (1988)

8. ábra. A Margala Hills, Potwar, Salt Range és a Hazara szintaxis egyszerűsített földtani térképe CALKINS & OFFIELD (1974), BOSSART et al. (1988), BURG et al. (2005), QAYYUM et al. (2015) és GHAZI et al. (2014) nyomán, S. AHMAD kézíratos térképét felhasználva

PKF = Panjal-Khairabad Fault; MBT = Main Boundary Thrust; KMF = Khari Murat Fault; KCR = Kala Chitta Range. Későbbi ábrák helyszíne vékony szaggatott vonallal. A Hazara-ív körüli vastag vörös pálcák deformációs ellipszoidok hossz tengelyeit jelölik BOSSART et al. (1988) alapján

a series of pop-up structures (BURG et al. 2005, their Figure 3) with relatively small allochthony.

Pre-Miocene rocks are overthrust towards the south onto the (Oligo-)Miocene molasse along the Main Boundary thrust (TREOLAR et al. 1992, BURG et al. 2005). The amount of overthrust is debated: in the order of 100km (TREOLAR et al. 1992) or just a couple of tens of km (BURG et al. 2005).

MBT may have different dips: it can be locally subvertical or even overturned, as also documented by BURG et al. (2005, their Figure 3) and our own observations. MBT runs at the northern outskirts of Islamabad, where it is expressed as the sudden rise of the mountain belt. Further east the topographic expression is less pronounced. However, east of Murree city MBT turns to north and then to NNW–SSE orientation, where it is called Murree Fault and forms a sharp, subvertical surface with oblique-horizontal scars along the boundary to the Oligo-Miocene (Figure 8; BURG et al. 2005). General understanding (KAZMI & RANA 1982, BOSSART et al. 1988) suggests that the N–S portion of the fault (Murree Fault) is in fact a lateral ramp, linking the frontal parts of Margala Hills to the northern thrusts of Hazara syntaxis.

2) On the surface the NPDZ (Figures 2, 8) is characterised by vast exposures of the Murree and Kamliyal Formations (Figure 3), the oldest terms of Miocene molasse. These are frequently crossed by ENE–WSW striking thrusts and are affected by ENE–WSW axial direction folding (Figures 8, 9). A narrow long belt of similar orientation made of a major Eocene cored fold, the Khari

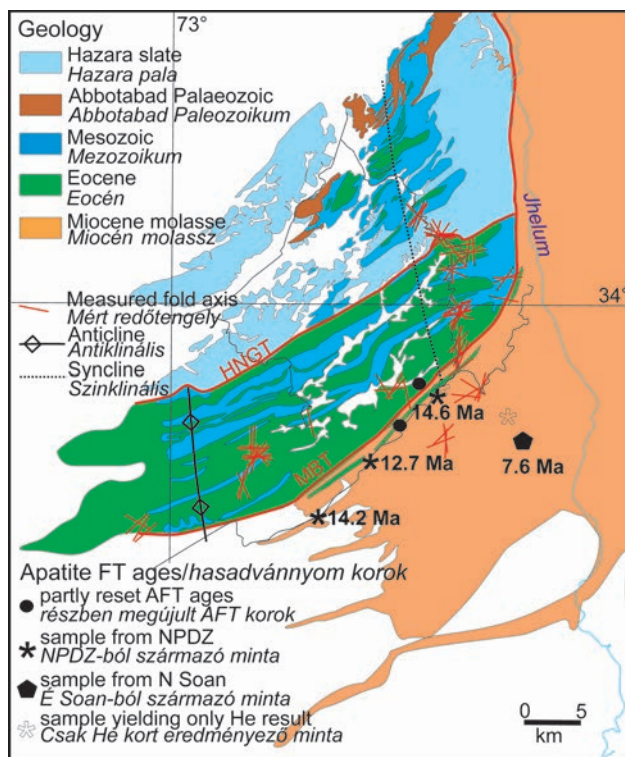


Figure 9. Simplified geological map of the Margala Hills and immediate southern foothills after LATIF (1968), incorporating a manuscript map of S. AHMAD

HNGT = Hazara-Natia Gali Thrust; MBT = Main Boundary Thrust. Red sticks mark own fold axis measurements; data collected by L. CSONTOS, Á. SASVÁRI, T. POCSAI, L. KÓSA. Note the presence of N–S trending outcrop-scale folds. Same lithology key as for Figure 2

9. ábra. A Margala Hills és közvetlen déli előtere egyszerűsített földtani térképe.

HNGT = Hazara-Natia Gali Thrust; MBT = Main Boundary Thrust; A vörös vonalak feltárásokban mért redőtengelyeket jelölnék by CSONTOS L., SASVÁRI Á., POCSAI T., KÓSA L. mérései alapján. Megjegyzendő az É-D-i tengelyű redők jelenléte. A közet-jelkulcs megegyezik a 2. ábrával

Murat Range, is exposed in the middle of this zone (Figures 2, 8). Taking subsurface information (just west of our Figure 10) into consideration NPDZ was described as a stack of imbricates or a duplex structure by JASWAL et al. (1997, their Figure 7), JADOON et al. (1997). The zone is formed by thin slices of the Cambrian–Eocene succession together with their Miocene cover; however, the same authors also suggest some detachment within the Miocene. A very similar structure was described across the Khari Murat Range by JADOON et al. (1999). However, the proposed imbricates beneath the exposed Khari Murat Range were subsequently not confirmed by drilling. All authors dealing with NPDZ suggested the existence of a major backthrust on the northern limb of the Soan syncline. This should have acted as a hangingwall-backthrust to form a triangle zone beneath (JASWAL et al. 1997, JADOON et al. 1999).

3) Salt Range is a long and wide set of Cambrian–Palaeozoic–Eocene exposures, onlapped by Late Miocene–Pliocene, locally Pleistocene molasse (JOHNSON et al. 1982, GRÉLAUD et al. 2002, QAYYUM et al. 2015). On the northern back-limb the Late Miocene–Pliocene forms the gentle Potwar Plateau, taken into local folds; the latter being more and more frequent towards the east (Figure 8). The huge Soan syncline forms the northern regional structure to this area. The southern edge is built of an escarpment made mostly by the Cambrian Salt Range formation and its Palaeozoic cover. The basal shear zone is composed of salt (GRÉLAUD et al. 2002 and references therein). This basal shear zone terminates east of Khewra as a dead-end (QAYYUM et al. 2015; Figure 8). The Palaeozoic–Eocene exposures are closed by a complex set of exposures. The eastwards end of Salt Range is apparently flexed towards the NNW into the Chambal Range (Figure 8) then it is flexed towards the NE (TREOLAR et al. 1992, QAYYUM et al. 2015), some flexing being supported by palaeomagnetic data (TREOLAR et al. 1992). The structure was analysed in detail by QAYYUM et al. (2015). According to their interpretation, the transversal Chambal segment was formed along a local lateral ramp oblique to the main Salt Range thrust. These authors also mention the Pabbi Fault (Figure 8) that runs in due continuation of the Salt Range trend but does not expose the older strata.

There is a set of NE–SW trending tight folds composed of Late Miocene–Pliocene formations on the eastern margin of this area. These structures were intensely explored for Petroleum (JADOON et al. 2015, their Figure 1). These were interpreted as deep imbricates or duplexes, similar to other parts of the NPDZ, although their transpressional character was also recognised (e.g. QAYYUM et al. 2015, their Figure 10). The core of these folds is composed of Cambrian–Eocene strata, overlain by Miocene molasse. However, at least one detachment within the Miocene is possible and locally active; therefore the folds at surface do not necessarily fully represent the structure at depth (Figure 8).

4) The Hazara syntaxis has a curvilinear shape with an ENE–WSW oriented northernmost portion (CALKINS & OFFIELD 1974, BOSSART et al. 1988; Figure 8). There are two thrusts parallel to each other, but both affect the same

lithostratigraphic units with identical, weakly metamorphic Permian–Early Mesozoic rocks, mostly volcanites. CALKINS & OFFIELD (1974) defined a small unit in the NE corner of the syntaxis that exposes Mesozoic rocks with Margala affinity. This zone was described by BOSSART et al. (1988) as a ‘mélange’ zone, with the understanding of a sheared unit of Mesozoic rocks (Figure 8). As opposed to the overlying Permian–Early Mesozoic, this unit might belong to a different structural unit (see later).

All around the syntaxis crystalline and Mesozoic rocks are thrust centripetally inwards over an Oligo–Miocene anchimetamorphic clastic succession (CALKINS & OFFIELD 1974, BOSSART et al. 1988; Figure 8). The originally interpreted Eocene ages of this molasse (BOSSART & OTTIGER 1989) were later re-examined and because of younger radiometric ages NAJMAN et al. (2002) reinterpreted the onset of Molasse sedimentation to not earlier than 25 Ma (Late Oligocene). The anchimetamorphic, cleaved clastic material in the centre gradually passes southwards to non-metamorphosed Lower Miocene Murree Molasses of the NPDZ. Near Muzaffarabad the molasse is underlain by Palaeogene and older rocks that are very similar to those exposed in the Margala Hills (BOSSART et al. 1988; Figure 8). This Palaeogene is uplifted along the SW-verging Balakot Thrust fault and is taken into an asymmetric fold, suggesting a top-SW transport (BOSSART et al. 1988).

BOSSART et al. (1988) measured strain ellipsoids in reduction spots of the Murree Formation. They suggested that deformation observed in the Murree Fm relates to a cigar-shaped strain ellipsoid with subvertical elongation and with a main flattening surface trending NNW–SSE. The two shortening axes were oriented ca NNW–SSE and ENE–WSW. Based on their strain measurements they suggested massive ENE–WSW shortening within the syntaxis, resulting in ductile folding of the Murree Formation.

They also measured strain ellipsoids mostly in the amygdaloids of Permian basalt in the overthrust nappes above the Murree Fm (Figure 8). These markers (that are born under weakly metamorphic conditions) seem to be parallel with the main local thrust and may be indicating shortening perpendicular to the main thrust surfaces. In the northern portion, where the chain turns ENE–WSW, these strain markers also seem to turn, although some depart from the exact trend of the main thrust fault. They interpreted this pattern as an indication of top SW and top SSE shear.

Own observations

A regional dip line across the Margala Hills–NPDZ area until the Soan syncline is presented (Figure 10). Two wells of more than 4 200 m (northern well) and 5 300 m (southern well) are projected from 5 and 6 km into the section. The northern well went through multiple repetitions of the Eocene–Mesozoic succession: after encountering a topmost normal then overturned succession of Eocene–Cretaceous of ca 1 300 m thickness, it drilled a normal sequence of Eocene marl and subordinate limestone with Palaeocene

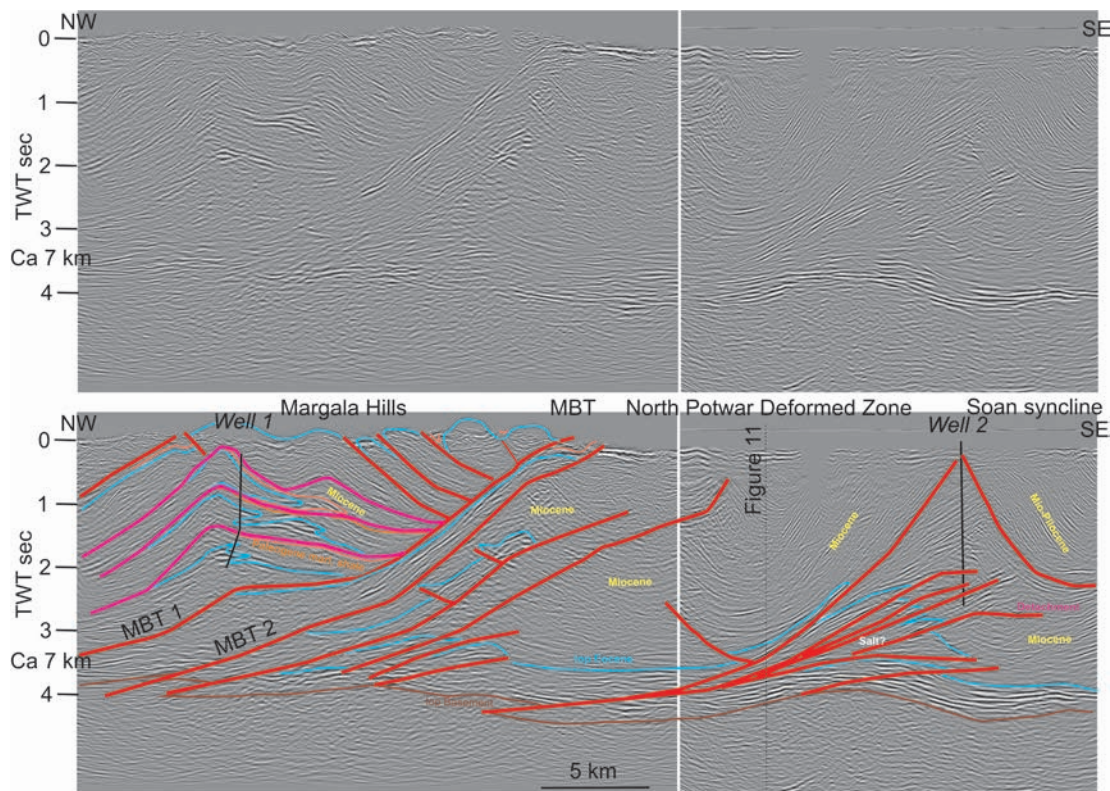


Figure 10. 2D seismic time section across Margala Hills and North Potwar Deformed Zone, uninterpreted and interpreted versions. MBT = Main Boundary Thrust. For location see Figure 8. Yellow indicates Miocene bed

10. ábra. Szeizmikus szelvény a Fő-feltolódással párhuzamosan, attól délre. A szelvény nyomvonal a 10. ábrán szerepel. Ugyanaz a színek, mint a 7. ábrán. A sárga egy miocén reflektort jelöl

shale of ca 650 m thickness, then again a normal sequence of Eocene–Cretaceous of ca 1 500 m thickness with Palaeocene shales at bottom of this section in a potentially overturned position; finally a disturbed succession of Eocene marl and a repetition of thin units of Palaeocene shale, limestone and thin Cretaceous (ca 600 m thick). Steep dips with often chaotic pattern characterised the whole drilled section. This fact together with the many potentially overturned sections suggest that the whole drilled assemblage is composed of tight, flat-lying folds. This is compatible with observations at surface (see the outcrop pattern on Figure 9).

When comparing the well section to the seismic a strong disharmony is observed. The tight, recumbent folds might not be imaged by seismic because of technical limitations, however, the steep dips should be somewhat displayed. Instead, one finds rather continuous sets of reflectors forming a major antiformal stack (the core of which was drilled). There might be two approaches: a) the seismic is totally irrelevant and shows only artefacts; b) the seismic shows basic units and structures, however cannot resolve the small-scale perturbations experienced by the well. Since the seismic pattern is rather consistent throughout the Margala Hills area, we believe rather the second option is true. Therefore, the interpretation is adjusted to symbolically indicate the tight, flat folds which are themselves apparently re-folded into a major antiform.

Because of the sharp breaks and thrust faults observed in the northern well and also because of the excessive thickness of drilled sediments compared to the reduced original thickness, it is necessary to introduce large thrusts between the individual drilled successions. We believe at least 4 imbricate sheets are documented by the well (separated by violet thrust surfaces on Figure 10). The uppermost one was not drilled, but projects above the well sequence. It is interesting to note that the highest sheet has a high thickness near MBT because of multiple possible repetitions along south-dipping back-thrusts. Because of thickness relations, it is possible that a small wedge of Miocene molasse is also captured beneath the topmost imbricate. All these imbricate sheets are folded into the antiform. The lowermost imbricate is underlain by a major ramp-flat thrust that can explain formation of the antiformal stack. This fault cuts up to the mapped MBT trace, therefore it is suggested that this is indeed a branch of MBT. Large overthrust of minimum 20 km is proposed along this branch alone.

Below the described antiformal stack lies a rather tabular body indicated by continuous, strong reflections (Figure 10). Near surface, this unit projects to Upper Eocene units immediately south of MBT (Figures 8, 9). Towards the west this unit continues in the Kalachitta Range (Figure 8), yet another mountain with Margala Hills affinity Mesozoic. It is therefore proposed that the tabular body is in fact another branch of MBT, with considerable (ca 15 km) minimal offset.

Several other tabular units along steeper thrusts can be interpreted immediately beneath these branches of MBT (Figure 10). These may cut upwards from a smaller duplex structure at depth, however, the seismic definition of the latter is far from clear. These imbricates may explain some of the thrusts cutting through the Miocene section in this part of NPDZ (Figure 8). From the section it is not clear whether the thin Cambrian–Eocene succession is underlain by salt or not.

Further south the second well targeted a triangle zone proposed by JASWAL et al. (1997), JADOON et al. (1999) (Figure 10). In spite of the presence of strong reflectors in an antiformal pattern the well drilled only repeated Miocene molasse sediments; therefore this hypothesis needs some modification. Interpreting the section, a gentle upwarp is experienced at Basement and its immediate reflective Cambrian–Eocene sedimentary cover. However, this structure might be uniquely due to velocity-pull-up. The reflections above this warp are arranged in a fan-like pattern, very similar to the one interpreted in NPDZ by JASWAL et al. (1997). It is believed that this fan indicates an imbricate structure of Cambrian–Eocene sediments floating above a reflection-free zone that possibly represents the Cambrian salt sequence (Figure 10). In summary, an imbricate stack does seem to exist, however, it does not reach as high as

proposed by earlier authors (JASWAL et al. 1997, JADOON et al. 1999). North and south of this structure two synclines are imaged in the Miocene succession. While the northern seems to conformably overly the proposed Eocene reflector, the southern one that is the Soan syncline seems to be detached from the Eocene along at least one detachment within the Miocene (Figure 10). Further, the reflection pattern also confirms the hangingwall-backthrust along the northern limb of Soan syncline, proposed by JASWAL et al. (1997) and JADOON et al. (1999).

A regional E–W 2D seismic line (Figure 11) parallel and immediately to the south of the MBT shows the E–W structure of the NPDZ until the supposed trace of Jhelum Fault (latter not being covered by the section). The topography rises towards the east, while the basement and its Cambrian–Eocene sedimentary cover (strong reflections near the base of section, Figure 11) seem to undulate and gently subside towards the east. Moreover, in the eastern portion of the line, westwards dipping reflectors within the basement suggest a set of east-vergent thrusts/imbricates within the basement. The section indicates that major folds with N–S axial trace do exist in the young Miocene cover (Figure 11). Some of those may be just oblique sections of top-south imbricates, but there are some that are clearly imaged by the Eocene reflector as well.

Together with topography Miocene horizons are also uplifted towards the east (Figure 11). These undulating horizons are then truncated by topography, so their uplift should have been even more important than the uplift deduced from topographic elevation. The geometry of eastwards subsiding basement and overlying Cambrian–Eocene cover and Miocene is not conformable (Figure 11). In other words, the upper and lower structures are clearly detached, and indeed there are multiple potential detachment horizons within shaly sequences of Miocene molasse. The space problem between the eastwards rising Miocene and eastwards subsiding Eocene basement may be resolved by a triangular shaped body, that could be a tectonically inserted excess mass of Miocene molasse, indicated by yellow shading on Figure 11. This mass could ride a west-vergent blind thrust (see later).

N–S axial trace folds can be also inferred from map analysis.

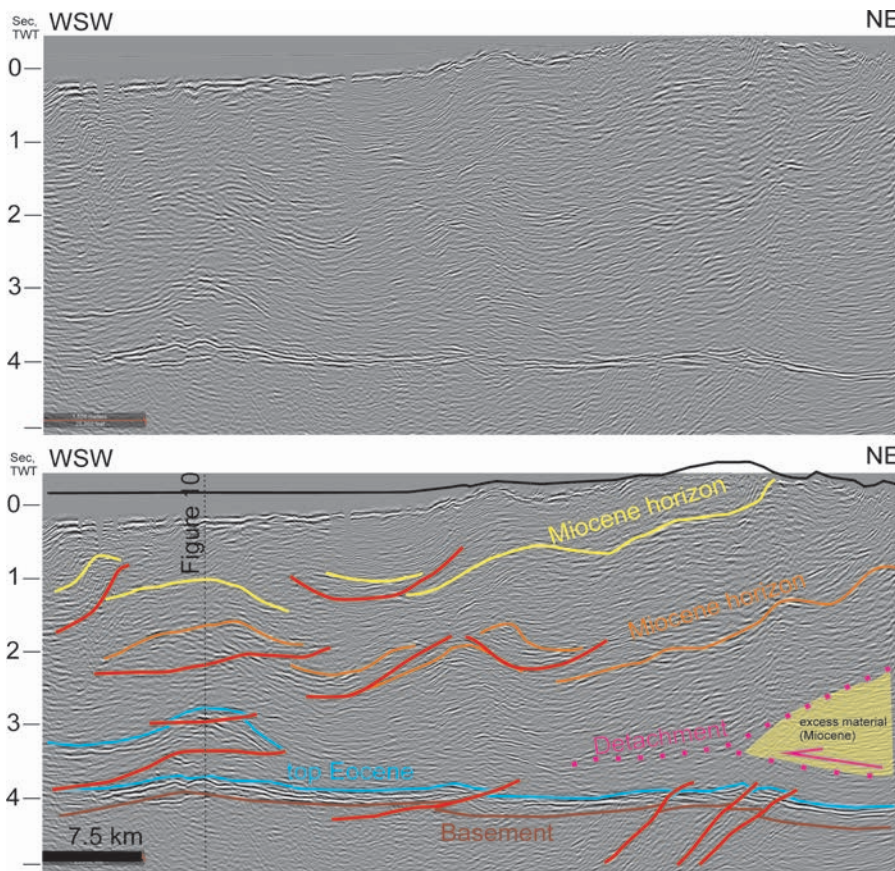


Figure 11. 2D seismic time section parallel to and south of Main Boundary thrust in North Potwar Deformed Zone, uninterpreted and interpreted versions. MBT = Main Boundary Thrust. Orange and yellow indicate different Miocene horizons. For location see Figure 8

11. ábra. Szeizmikus szelvény a MBT feltolódással párhuzamosan, attól délre. Narancssal és sárgával különböző miocén szinteket jelöltünk. A szelvény nyomvonala a 8. ábrán látható

Margala Hills shows four way closed anticlines at its western portion (Figures 8, 9). They are aligned on a N–S trend and this trend also continues at subsurface, at a set of imbricates (Figure 8, southern-central part) that are also folded in an E–W direction (see the anticline in top Eocene Figures 8, 11). Another N–S trending anticline may be outlined further east, but its trace is not as certain as the previous one (Figure 8). Finally a regional N–S syncline can be proposed in the Hazara–Natia Gali thrust unit, where Mesozoic is preserved in a four way closed synclinal zone (Figure 9).

Figure 8 shows structures at surface and subsurface. Naturally, this cannot reflect all the subsurface structures, because parts of the area are not accessible, adequate seismic material is not available or simply not known to us. However, the displayed subsurface structures seem to be on trend and following the surface structures, most importantly the anticlines within Miocene molasse. However, structures at depth are characterised by S–SE vergent main thrusts frequently accompanied by conjugate, smaller offset NE-vergent backthrusts. The long, persistent anticlines in Miocene often hide a set of relaying structures at depth (Figure 8). These features suggest that important strike slip component was added to the general thrust (GRÉLAUD et al. 2002, BURG et al. 2005, QAYYUM et al. 2015).

The map (Figure 8) also suggests that the structures at the eastern edge of Potwar Plateau apparently continue across the Jhelum river and western Kashmir towards the east. Subsurface information is quite reduced in this area, however, based on mapping several NE–SW axial trace folds in Potwar are re-folded and continue without a break along a NW–SE trend in Kashmir.

The regional Jhelum strike slip fault (Figure 2) is

proposed to link the N–S trending Murree Fault (Figure 9; western limit of Hazara syntaxis) to the eastern termination of Salt Range Thrust (KAZMI & RANA 1982, CRAIG et al. 2018) and should act as a lateral ramp. The small, local Chambal lateral ramp (QAYYUM et al. 2015) does not continue northwards and cannot be part of this Jhelum Fault; moreover, it has NW–SE orientation (Figure 8). The proposed Jhelum Fault trace should cross many of the shown subsurface structures, yet there is no trace of a regional, cross-cutting fault in the given zone. The regional Jhelum Fault could run along the Jhelum river itself, but in that case it would not explain the termination of Salt Range Thrust. Nevertheless, it should dissect many of the surface structures between Potwar and Kashmir, which is not observed either. In short, the supposed Jhelum Fault cannot be proven and is not compatible with observations. On the other hand, small scale folds, as well as regional folds of N–S axial trace orientation are present throughout the area. In the Jhelum region, apparently earlier folds are re-folded to form a series of folds with N–S axial trace (Figure 8).

Low-temperature thermochronology

Apatite fission track and (U–Th)/He measurements were applied on samples from different elevations and different structural settings from the Murree Fm (Figure 9). Sample locations are shown on Figure 9, the mean age vs. elevation plot and the raw analytical data are presented on Tables I, II and Figure 12. For the evaluation of the low-T age data we should consider that the depositional ages of the siliciclastic samples are between 25 and 18 Ma. Except two ages (see below) the apparent ages of the apatite fission

Table I. Apatite fission track results obtained on the sandstone samples of Murree Formation

I. táblázat. Apatit hasadvány nyomok a Murree Formáció homokkövein mérve

Sample	Northing	Easting	Elev. [m]	Crystal	RhoS	[Ns]	RhoI	[Ni]	Chi-sq. P (%)	Disp.	Central Age	±	Is
MMr-1	33° 45.19'	73° 12.26'	613	20	3.246	[232]	21.815	[1559]	7	0.25	17.4 ± 1.7		
MMr-1				16*	1.998	[121]	17.274	[1046]	95	0.00	14.2 ± 1.4		
MMr-3	33° 49.00'	73° 16.43'	828	20	3.861	[274]	24.601	[1746]	0	0.56	18.6 ± 2.8		
MMr-3				16*	2.163	[131]	21.139	[1280]	99	0.00	12.7 ± 1.2		
MMr-6	33° 51.52'	73° 19.37'	1322	20	4.079	[239]	21.677	[1270]	1	0.29	22.8 ± 2.4		
MMr-8	33° 54.48'	73° 20.48'	1853	11	5.439	[247]	17.814	[809]	0	0.30	34.2 ± 4.2		
MMr-11	33° 53.22'	73° 22.38'	1990	20	2.859	[251]	19.879	[1745]	0	0.33	16.0 ± 1.7		
MMr-11				19*	2.481	[208]	19.38	[1625]	77	0.00	14.6 ± 1.2		
02-11	33° 50.605'	73° 28.184'	1720	20	1.406	[160]	13.555	[1543]	0	0.46	11.9 ± 1.7		
02-11				15*	0.769	[65]	12.243	[1035]	97	0.00	7.6 ± 1.0		
02-11				5	3.243	[95]	17.342	[508]	81	0.00	22.5 ± 2.6		

Locations are given in degrees and decimal minutes, see also Figure 9. Lines typed in Italics show data considering all crystals. *: Indicates isolated groups of data measured on crystals having similar composition and closure temperature. Track densities (Rho) are as measured ($\times 10^5$ tr/cm²); number of tracks counted (N) shown in brackets. Track densities and track numbers in the CN5 detector: 6.10 [2937]. Chi-sq P(%): probability obtaining Chi-square value for n degree of freedom (where n = no. crystals-1). Disp.: Dispersion, according to GALBRAITH & LASLETT (1993). Central ages calculated using dosimeter glass: CN5 with zeta CN5 = 373.3 ± 7.1

A minták helyzete fokokban, decimális percekben vannak megadva (lásd még 9. ábra). A dőlt betűvel szedett részek az összes kristályra vonatkozó adatokat tartalmazzák. *: azonos összetételű és záródási hőmérsékletű kristályokon mért adatok. A nyomsűrűsége (Rho) $\times 10^5$ tr/cm²-ként szerepel a nyomok számát (N) zárójelben mutatjuk. A CN5 detektoron mért nyomsűrűség és nyomszám: 6.10 [2937]. Chi-sq P(%): a chi-négyszertest eredménye n szabadsági fok esetén (ahol n = a datált kristályok száma-1). Disp.: GALBRAITH & LASLETT (1993) szerinti diszperzió. A centrális korokat CN5 doziméter segítségével zeta CN5-el (373.3 ± 7.1) számoltuk ki

Table II. Apatite (U–Th)/He results obtained on single crystals from sandstone samples of the Murree Formation
II. táblázat. Apatit (U–Th)/He eredmények, melyeket a Murree Homokkő egység kristályain mértek

Sample	Northing	Easting	Elev. [m]	Aliq.	He [ncc]	He unc. [fs, ncc]	U [ng]	U unc. [fs, ng]	U ppm	Th [ng]	Th unc. [fs, ng]	Th ppm	Th/U [ppm]	Sm [ng]	Sm unc. [fs, ng]	Sm ppm	Apatite [µg]	Uncorr. age [Ma]	Ft	Corr. Age [Ma]	unc. [±s, Ma]	Sample aver. & s.d. [Ma]
MMr-1	33°45.19'	73°12.26'	613	#2	0.089	0.002	0.131	0.003	41	0.161	0.004	50	1.2	0.21	0.01	66	3.2	4.3	0.83	5.2	0.3	4.4 ± 1.1
					0.017	0.001	0.011	0.003	5	0.190	0.005	88	17.5	0.13	0.00	61	2.2	2.4	0.79	3.1	0.4	
					0.028	0.001	0.022	0.002	6	0.136	0.003	37	6.2	0.59	0.02	159	3.7	3.9	0.80	4.9	0.6	
MMr-3	33°49.00'	73°16.43'	828	#2	0.034	0.001	0.030	0.003	12	0.186	0.005	75	6.1	0.30	0.01	120	2.5	3.6	0.88	4.1	0.4	4.8 ± 1.5
					0.118	0.002	0.168	0.004	94	0.115	0.003	64	0.7	0.49	0.01	271	1.8	4.9	0.74	6.6	0.3	
					0.093	0.002	0.177	0.004	44	0.470	0.011	118	2.7	1.19	0.07	297	4.0	2.6	0.69	3.8	0.2	
MMr-6	33°51.52'	73°19.37'	1322	#1	0.153	0.002	0.662	0.012	88	0.035	0.001	5	0.1	2.23	0.06	295	7.6	1.8	0.82	2.3	0.1	4.3 ± 2.9
				#2	0.329	0.003	0.546	0.010	218	0.040	0.001	16	0.1	0.82	0.02	328	2.5	4.8	0.76	6.3	0.3	
MMr-8	33°54.48'	73°20.48'	1853	#1	0.248	0.003	0.285	0.006	65	0.488	0.012	111	1.7	0.31	0.01	70	4.4	5.1	0.82	6.2	0.2	5.1 ± 1.6
				#2	0.087	0.002	0.084	0.003	20	0.542	0.013	130	6.5	0.49	0.01	119	4.2	3.3	0.83	4.0	0.2	
MMr-9	33°53.23'	73°21.47'	1708	#1	0.027	0.001	0.025	0.002	22	0.126	0.003	113	5.1	0.40	0.01	357	1.1	3.9	0.55	7.1	0.8	
MMr-11	33°53.22'	73°22.38'	1990	#3	0.032	0.001	0.068	0.003	58	0.131	0.003	112	1.9	0.41	0.01	348	1.2	2.6	0.64	4.1	0.4	4.5 ± 0.5
				#4	0.047	0.001	0.026	0.002	27	0.387	0.009	393	14.7	0.34	0.01	345	1.0	3.2	0.74	4.4	0.3	
				#5	0.107	0.002	0.068	0.002	34	0.617	0.015	308	9.0	0.62	0.03	311	2.0	4.0	0.80	5.1	0.3	
02-08	33°51.701'	73°27.787'	1636	#1	0.110	0.002	0.162	0.003	23	0.509	0.012	72	3.1	1.35	0.11	190	7.1	3.1	0.85	3.6	0.2	2.9 ± 0.6
				#2	0.734	0.006	2.005	0.036	164	2.548	0.061	209	1.3	1.19	0.10	98	12.2	2.3	0.85	2.7	0.1	
				#3	0.020	0.001	0.046	0.002	42	0.255	0.006	234	5.6	0.08	0.01	78	1.1	1.6	0.64	2.4	0.2	
02-11	33°50.605'	73°28.184'	1720	#1	0.126	0.002	0.209	0.004	49	0.570	0.014	134	2.7	0.27	0.01	65	4.3	3.0	0.81	3.7	0.2	3.5 ± 0.2
				#2	0.039	0.001	0.088	0.003	28	0.159	0.004	51	1.8	0.18	0.01	57	3.1	2.6	0.78	3.3	0.3	
				#3	0.032	0.001	0.073	0.003	58	0.090	0.002	72	1.2	0.29	0.01	228	1.3	2.8	0.76	3.6	0.3	
KCS-2	33°53.252'	73°22.256'	1960	#1	0.180	0.003	0.226	0.004	21	0.455	0.011	42	2.0	2.00	0.17	184	10.9	4.3	0.82	5.2	0.2	4.7 ± 1.2
				#2	0.069	0.002	0.201	0.004	83	0.157	0.004	65	0.8	0.57	0.05	236	2.4	2.4	0.71	3.3	0.2	
				#3	0.124	0.002	0.135	0.003	41	0.388	0.009	117	2.9	0.72	0.06	216	3.3	4.4	0.79	5.6	0.3	

Locations are given in degrees and decimal minutes, see also Figure 9. Amount of helium is given in nanocubic-cm in standard temperature and pressure. Amount of radioactive elements are given in nanograms. Ejection correct. (Ft): correction factor for alpha-ejection (according to FARLEY et al., 1996). Uncertainty of the single grain age is given as 2 sigma in % and it includes both the analytical uncertainty and the estimated uncertainty of the Ft.

A minták helyzete fölökben, decimális percekben vannak megadva (lásd még 9. ábra). A He mennyiségét standard hőmérsékleten és nyomáson mérve nanoköb-cm-ben adjuk meg. A radioaktív elemek mennyiségét nanogrammban adjuk meg. A kilöködési korrekciót FARLEY et al. (1996) módszere alapján számoltuk. Az egyes korok hibáját 2 szigma-ként adjuk meg, amely tartalmazza mind a propagált analitikai hibát, mind a kilöködési korrekció hibáját.

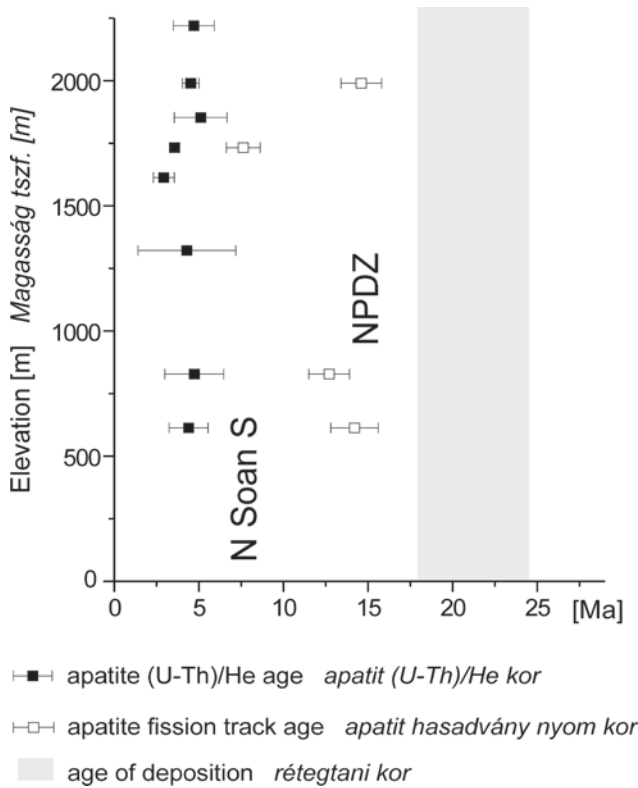


Figure 12. Apatite fission track and (U-Th)/He ages against sample elevations in the Murree Formation (see raw data in *Tables I, II*). Location of samples on *Figure 9*

N Soan S = Northern margin of Soan syncline continuation. NPDZ = North Potwar Deformed Zone

12. ábra. Apatit hasadványnyom és (U-Th)/He korok a Murree Formációból vett mintákon, az I és II táblázat adatai nyomán. A mintavételi helyek a 9. ábrán szerepelnek

N Soan S = A Soan szinklinális északi szegélyének folytatása; NPDZ = North Potwar Deformed Zone

track and (U-Th)/He thermochronometers are younger than the stratigraphic ages, thus these constraints indicate obviously a post-depositional thermal overprint. Assuming ca 10 Myr long effective heating time the maximum temperature was around 120 °C (e.g. REINERS & BRANDON 2006). Much higher overprint temperature is not probable, as some detrital apatite grains show larger Dpar values suggesting that a part of the detrital apatite crystals have higher closure temperature (BURTNER et al. 1994) and this fraction of grains shows only incomplete fission track reset.

The localities of the samples used for low-T thermochronology are presented in *Figure 9*. Two samples from the Miocene molasse of the Margala Hills unit, very close to MBT, three samples from the NPDZ immediately to the south of MBT, and one sample from the northern limb of the continuation of regional Soan syncline yielded interpretable apatite fission track ages. The northernmost two samples showed only partial reset — in these cases the sample means are older than age of sedimentation — indicating that the Margala Hills unit was not deeply buried enough and for a sufficient time to result in reset. These samples are not illustrated on *Figure 12*.

In the samples from the NPDZ the apatite FT thermochronometer experienced complete reset and showed Middle Miocene ages between 14 and 12 Ma and a slight dependency with topographic height (*Figures 9, 12*). These ages indicate that uplift of the imbricate system in the NPDZ started in Middle Miocene and possibly MBT was also active in Early (?)–Middle Miocene times. The southernmost sample at the northern limb of the continuation of Soan syncline was also completely reset and showed Pliocene cooling age of 7 Ma (*Figures 9, 12*). This indicates that the hangingwall backthrust of JASWAL et al. (1997) and JADOON et al. (1999) and, consequently the southern advance of the NPDZ imbricate wedge at its base lasted at least until Pliocene. Overall, the apatite fission track ages indicate a southwards younging of uplift that is in good agreement with general, local development of the mountain system (e.g. TREOLAR et al. 1992). The new information suggested by our measurements is that this southwards propagation should have started earlier than proposed (ages around 10 Ma for MBT activity; see TREOLAR et al. 1992, BURG et al. 2005). It is also important to note that GRÉLAUD et al. (2002) already suggested earlier deformation ages and the initiation of the southernmost Salt Range thrust as early as 8.8 Ma.

The apatite (U-Th)/He ages (*Table II, Figure 12*) yielded an average of ca 4 Ma and the data show less scatter than the fission track ages. Remarkable is that the helium ages show practically no age-elevation dependence. This suggests a fast exhumation event that could be coincidental with the eastwards rise of Margala Hills and the area near Murree city (see the eastern part of *Figure 11*). It is proposed that this sudden uplift can be coincidental with the formation of the Hazara dome and related thrusts.

Discussion

1. Main Boundary Thrust

As remarked by TREOLAR et al. (1992), MBT is rather a swarm of different shear planes than a single shear plane. Our data also indicate that MBT should be composed of different, shorter segments that relay each other. Such relays can be seen at several locations and are indicated on *Figures 2 and 8*, one is found immediately west of Islamabad; another prominent relay is found north of Kohat city. The relays seem to be consistent with a left lateral transpressive motion. The offset along these individual thrust surfaces may vary; it should be in the order of 20 km (*Figure 10*); these offsets may add up to a cumulative offset of ca 70 km in the Hazara syntaxis (see also TREOLAR et al. 1992).

The eastwards continuation of MBT is in the Murree Fault. Based on observations of shallow-dipping slickenslide lineations, most authors (BOSSART et al. 1988, BURG et al. 2005) suggest that this is a major left lateral strike slip fault. Although we do not exclude late stage strike slip faulting, we would rather agree with TREOLAR et al. (1992) who suggest that Murree Fault is the bent segment of MBT and the

slickenlines indicate the original nappe emplacement above the Miocene molasse in the centre of Hazara syntaxis, i.e. an originally flat-lying MBT, turned into vertical on the limb of the major Hazara antiform (*Figure 2*; see later).

North of Muzaffarabad (*Figure 2*) the continuation of MBT is doubtful: most maps continue it along the southern thrust fault of Hazara syntaxis, below the ‘Panjal Imbricates’ of BOSSART et al. (1988). However, in this case MBT would carry a highly deformed, cleaved Permian volcanic sequence that is the characteristic lithology of the Panjal Thrust sheet. Therefore we propose that the Panjal-Khairabad thrust, a major nappe boundary, should rather run along the southern thrust fault of the Hazara syntaxis (i.e. south of the ‘Panjal imbricates’, see *Figure 2*) and the northern thrust fault (generally named as Panjal Thrust) should be just an internal repetition within the Panjal Thrust sheet (for simplicity not illustrated on *Figures 2, 8*).

If Panjal Thrust runs in the internal part of Hazara syntaxis, there are two possibilities to continue MBT: either buried beneath the Panjal Thrust (and therefore unseen), or to continue it along the Balakot Fault. The former solution (*Figure 13, a*) would profit of the observation of Jurassic–Cretaceous–Palaeocene lithologies described by BOSSART et al. (1988) as a tectonic mélange. These Mesozoic–Palaeogene elements are clearly related to Margala Hills and should not be part of the low grade metamorphic Panjal nappe with different composition. The mélange zone either indicates the tectonic contact of Panjal and Margala Hill nappes and sheared elements of both units, or an imbricate within the Margala Hill unit. In this latter case its lower boundary could be indeed an exposure of the buried MBT (*Figure 2*). In the second case (*Figure 13, b*), MBT would not continue northwards north of Balakot, but would turn sharply SE-wards along the Balakot Thrust (*Figures 2, 8*). This solution would be conformable to the tight fold pattern seen more to the south within the Miocene molasse (see analysis of east-Potwar, west-Kashmir), i.e. this solution would suggest that the MBT is itself tightly folded by NNW–SSE axial trace late fold (see later).

2. Main Frontal Thrust and Kalabagh Fault

Similar to MBT, the Main Frontal Thrust also seems to be composed of relaying elements. An obvious relay is found between the Makarwal segment and Kishor–Marwat Ranges (*Figure 2*); similar relays can be found between eastern termination of Surghar Range and the Kalabagh slice (*Figure 4*); eventually between the Kalabagh slice and the Gundi Lobe, between the Gundi and Mussa Khel Lobes (GHANI et al. 2018). Some relays seem to be consistent with left lateral, others with right lateral transpressive movement. If we accept that there are relaying tectonic slices and not a single unit along the MFT, there is no more need for a Kalabagh lateral ramp fault that cuts up and offsets this single unit; the different, separated exposures may form part of different imbricate sheets.

MFT eastern termination is interesting, because this fault seems to splay off into different segments. One of the splays is

the Domeli Thrust (*Figure 8*); another one continues along the complex Chambal ridge, yet another seems to continue towards the Pabbi fold (QAYYUM et al. 2015). As opposed to the other segments, Pabbi segment does not seem to suffer secondary deformation; it continues the ENE–WSW trace of the Salt Range Thrust. This might indicate that its generation post-dates major folding in the whole of Hazara syntaxis.

As earlier proposed, Kalabagh Fault imagined and drawn on many maps (KAZMI & RANA 1982, MC DOUGALL & KHAN 1990, GHANI et al. 2018) cannot be proved (*Figure 4*). However, the only segment that may really exist is found between the Kalabagh slice and the Gundi Lobe. The northwards continuation along Chisal Algad is a complex deformation zone without any through-going fault. However, if the whole structural assemblage is observed, a right lateral shear zone could be interpreted. *Figure 4* shows a set of ESE–WNW oriented steep, transpressive structures and arranged en echelon along a localised NNW–SSE trending zone. The folds along Chisal Algad are also arranged en echelon. Both are local structures that cannot be found elsewhere, and both fit a broader and more ductile N–S trending right lateral shear zone that also contains the southwards flexed Visor Fault, the southwards flexed Kalabagh slice and Cemetery Fault and in fact the whole Western Salt Range segment (*Figure 4*). In our opinion the main deformation along this zone is rather folding than faulting: earlier thrusts and imbricates are flexed southwards. In that interpretation the originally more linear and relaying MFT elements were later folded, flexed along the broad ductile shear zone with a right lateral component. It is also clear that formation of N–S trending folds and top-east thrusts preceded this ductile flexing/shearing, because different elements of the ductile flexing zone gradually disappear towards the west, on the eastern limb of the main N–S trending fold seen on the 3D cube and they also cut up the elements of the top-east thrusts (*Figure 4*).

3. E–W shortening

In the Himalaya foothills, N–S trending folds are present from Kohat Plateau to Potwar Plateau and beyond, into Kashmir. The whole region abounds in four-way closures (CRAIG et al. 2018) and most are not born of local modifications of the E–W trending main trust fault attitudes but they are the results of transversal folding. Such a transversal fold is clearly seen on the presented 3D cube (*Figures 4, 7*). Moreover, maps from the different mountain segments also suggest or indicate transversal folding (see *Figures 8, 9, 11*). The Miocene folds along the Jhelum river also seem to have formed in a more linear position and later re-folded along a major fold of N–S axial trace. This fold continues into the Hazara syntaxis (*Figure 8*).

Hazara syntaxis has been interpreted by many as a major antiform (BOSSART et al. 1988, TREOLAR et al. 1992, BURG et al. 2005, BURG & PODLADCHIKOV 1999), which is in full agreement with our views. This major antiform can also be extended to the southern foreland, along the flow of Jhelum river (*Figure 8*). As it was concluded earlier, there is no need

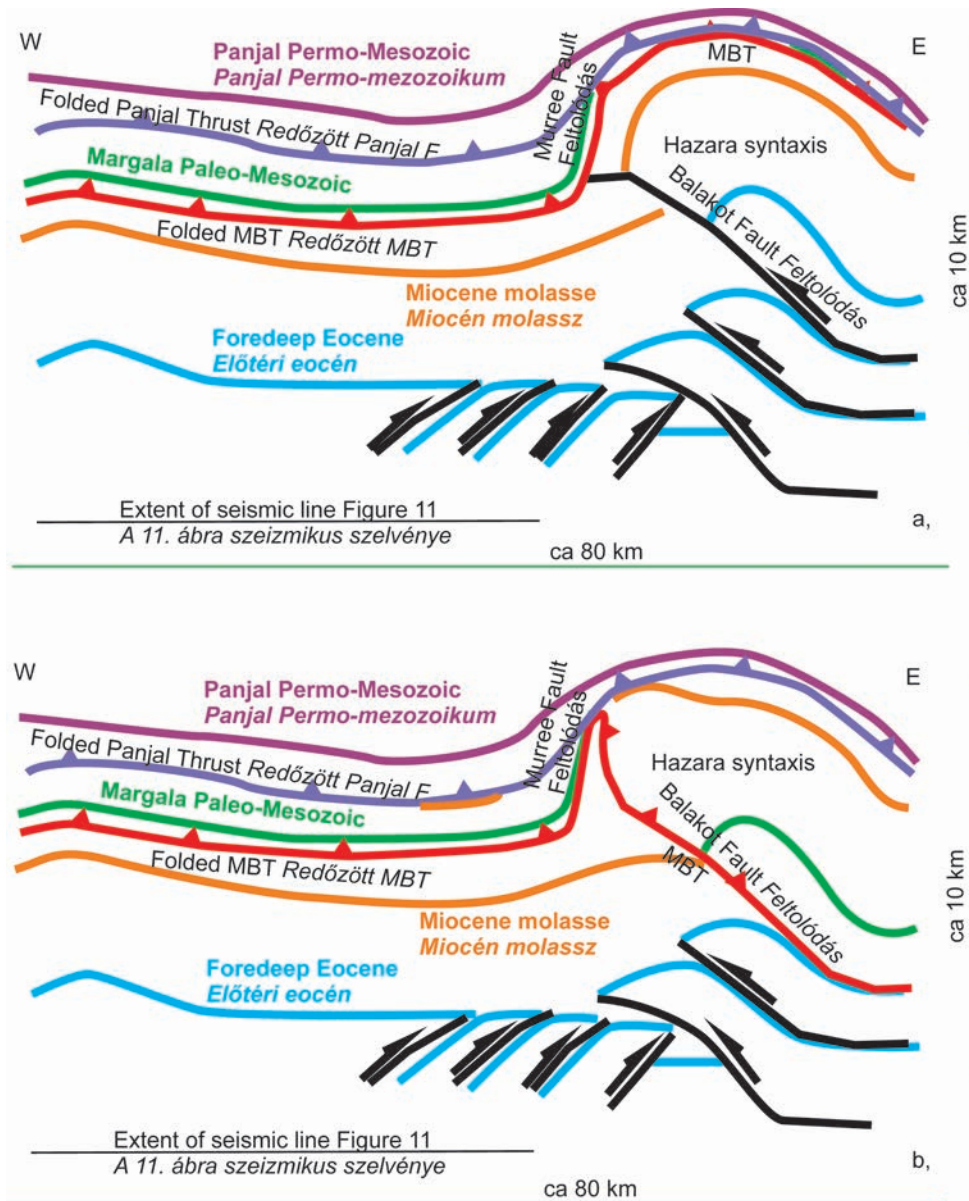


Figure 13. Schematic W-E cross section of the Margala Hills - Hazara syntaxis area. Without scale; approximate horizontal and vertical measures marked

a) MBT (Main Boundary Thrust) runs largely hidden beneath PKF (Panjal-Khairabad Faults). b) MBT is linked with Balakot Fault and is tightly folded

13. ábra. A Margala-hegység és a Hazara szintaxis vázlatos Ny-K-i szelvénye. Lépték nélkül, a nagyjából vízszintes és függőleges mértékekkel jelölve

a) Az MBT (Main Boundary Thrust) nagyrészt láthatatlanul elbújva közvetlenül a PKF (Panjal-Khairabad Faults) alatt található. b) MBT a Balakot feltolódásban folytatódik, szorosan meg van gyűrve

and no space to place a Jhelum Fault of major left lateral ramp character across eastern Potwar. Folding around the Hazara syntaxis may be indicated by measurements of strain ellipsoids in BOSSART et al. (1988). The flattening surface of their strain ellipsoids in the Panjal series was always parallel to the local attitude of main thrust surfaces; the main elongation direction was also parallel or slightly oblique to the strike of these main thrusts (Figure 8). The measured deformation pattern may be compatible with a more linear Panjal Thrust and a later folding of these strain

indicators along the Hazara antiform. That would suggest that thrusting along the Panjal Thrusts was preceding E-W shortening and Hazara antiform generation (TREOLAR et al. 1982). However, BOSSART et al. (1988) also indicated ductile structures on the back-limb of Muzaffarabad fold that are more E-W axial trace folds. Since these affect the mentioned fold in the core of Hazara antiform, they should be later structures (BOSSART et al. 1988).

Hazara syntaxis as a main antiform apparently contradicts an observation seen on Figure 11: the eastern part of

‘basement’ is subsiding, rather than being uplifted towards the core of that antiform. This observation can be extended to the whole Potwar Plateau, its eastern area being substantially deeper than the western one. The whole subsurface seems to be generally tilted towards the east. In our opinion this controversy can be resolved by proposing a series of west-vergent blind thrust that produce the needed wedge-shaped excess mass proposed on *Figure 11* to uplift the Murree–Hazara area. Two conceptual models are prepared (*Figure 13*), depending on the position of MBT; however, both suggest that the whole of Hazara syntaxis, with MBT and Panjal Thrust included, are folded above multiple west-vergent imbricates within the foothills (NPDZ), the Balakot Thrust being only one of these thrusts or the folded MBT itself.

In a greater context, the whole northern margin of Indian shield shows intense folding with N–S axial trace (*Figure 2*; DiPIETRO et al. 2008). The Indus syntaxis near Besham and the Nanga Parbat syntaxes are main examples (TREOLAR et al. 1992), but many other smaller amplitude domes with similar orientation do exist. These antiforms fold metamorphic rocks of different internal units. As observations and the map in DiPIETRO et al. (2008) suggest, initiation of domal uplift together with similarly oriented outcrop-scale folds (their F3 generation in DiPIETRO et al. 2008) should have occurred prior to the main movements of their Kohistan Fault (*Figure 2*), i.e. prior to 31 Ma in their opinion. However, several thermochronologic measurements (4 Ma apatite fission track ages in ZEITLER 1985) and observations of uplifted and faulted Quaternary sediments (DiPIETRO et al. 2008) suggest that at least one dome, the Indus syntaxis at Besham (*Figure 2*) is uplifted in Late Pliocene to Quaternary times (see also TREOLAR et al. 1992). The Nanga Parbat syntaxis is also uplifted in Plio–Pleistocene (ZEITLER 1985).

Folding of lithospheric scale was modelled by BURG & PODLADCHIKOV (1999). In their numerical model they varied the thermal structure, i.e. the rheology of the lithosphere and calculated its response to lateral (E–W) compression. The result was lithospheric folding. They found that their ‘warm’ (as opposed to ‘cold’ or ‘hot’) rheology was best reproducing the wavelength and amplitude of Nanga Parbat (s. str) syntaxis (antiform) and the parallel synforms that they proposed to be located in the Kashmir (Shrinagar) and Peshawar Quaternary basins (*Figure 1*).

4. Possible reasons for E–W shortening in a general N–S shortening context

BOSSART et al. (1988) interpreted their strain measurements as indicators of a first top-SW, then a second top-SSE shortening event. They proposed that the original trace of thrusts was much more linear, but because of the gradual change in main shear directions from top-SW to top-SE a curved aspect of the thrusts developed. In short, they developed the Hazara syntaxis with a gradually rotating southerly shear and with the interference of a ductile left lateral zone that they continued further south. Although

many of the observed structures are compatible with top SW shear, we believe that their observations can be also interpreted as later folding of an original syn-cleavage deformation along much more linear thrust faults. The gradually changing shear directions are also in conflict with main recent top-SW shear measured by episodic GPS positions (JOUANNE et al. 2014).

TREOLAR et al. (1992) proposed that fault terminations of a synchronous thrust system might produce a zone of roughly E–W convergence (*Figure 14, a, b*). NW–SE trending faults on the Kashmir side with top SW transport would terminate in a zone along Jhelum river. Differential transport along these faults (with zero transport at tips, maximum transport in the SE) would induce clockwise body rotations. Thrust faults with NE–SW orientation in Potwar and terminating also in the same zone along the Jhelum river would initiate counterclockwise rotations. Such opposed rotations are indeed observed in palaeomagnetic declinations measured in the area (KLOOTWIJK et al. 1981, BOSSART et al. 1988). These authors suggest that the Hazara syntaxis is the result of the interference of these two fault sets of different orientations, both having tip lines in a common zone. The result would be a N–S trending antiform without real and general E–W shortening.

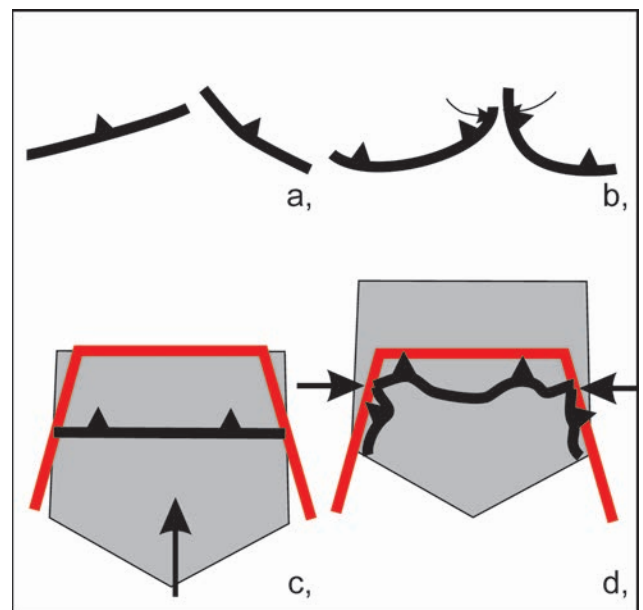


Figure 14. Simplistic models (map views) to explain E–W shortening in a general N–S shortening regime

a), b) Opposite rotations around fault terminations, after ideas of TREOLAR et al. (1992). Although map view is reproduced, the process does not generate regional E–W shortening. c), d) Northwards thrust along converging confining margins, after analogue experiments of REPLUMAZ et al. (2012). Original more linear E–W striking structures are refolded and east- and west-vergent thrusts, N–S trending folds are generated by induced E–W shortening

14. ábra. Egyszerűsített földtani modellek (térképi nézet) a másodlagos K–Ny-i rövidülés magyarázatára

a, b) Feltolódás-elvegződések menti egymással ellentétes forgások TREOLAR et al. (1992) gondolatai nyomán. Bár a térképi nézetet a folyamat reprodukálja, nem okoz regionális K–Ny-i rövidülést. c, d) Észak felé történő lemezmozgás két szűkülő oldalhatár mentén, REPLUMAZ et al. (2012) analóg kísérletei nyomán. Az eredeti, lineárisabb, K–Ny-i csapású szerkezetek meggyűrődnek, a határok mentén keleti és nyugati vergenciájú feltolódások és É–D-i tengelyű redők keletkeznek az indukált K–Ny-i rövidülés hatására

Since N–S trending folds seem to be general structural features in the whole of the Pakistani Himalayan area (at least south of Kohistan Fault, *Figure 2*), it seems to be very hard to explain these by fault terminations and opposed rotations, fault interference. We would rather believe that there is a genuine E–W shortening affecting the whole region under consideration.

REPLUMAZ et al. (2012) performed analogue modelling in which they looked for the possible reasons of E–W shortening in a general N–S shortening context. In their sandbox models they modelled a wedge-shaped indenter, confined laterally by northwards converging boundaries with softer cover rocks above more rigid basement rocks. They pushed the whole southern part, mimicking the northern margin of Indian continent northwards. As expected, the lateral confining boundaries produced imbricates (thrust mountain belts) parallel to their trends that had mostly inwards, i.e. E-vergent or W-vergent transport (*Figure 14, c, d*). The main frontal convergence was characterised by an E–W trending thrust belt. This model clearly demonstrated that an overall N–S convergence and shortening can effectively provide local and temporal E–W shortening due to the confining boundaries. In our case it is not important whether the confining boundaries modelled by REPLUMAZ et al. (2012) are well-chosen or not, the principle will hold. In our view the concept may be extended not only to the NW region of the Himalayas, but eventually to the whole of India, confined by the slightly converging Quetta–Chaman fault zone in the west and the Sagaing Fault in the east (*Figure 1, a*). Both should be lithospheric boundaries along which India progresses to the north (MOLNAR & TAPPONIER 1975).

In a second set of analogue experiments BAJOLET et al. (2013) modelled the dependency of mountain shapes on rheology of the overriding and subducting plates and the resistance on the subduction zone itself. Subducting plates contained both denser (oceanic) and lighter (continental) material. They wished to reproduce the two greater syntaxis areas at the NW and SE corners of the Himalayas (*Figure 1, a*). They found that if subduction is lubricated, i.e. with low resistance, substantial underthrusting will create an arcuate mountain range above the subducting slab with two syntaxial areas developed at each corner (thus reproducing the overall shape of the Himalayas). This shape did not depend much on the rheology and thickness of the upper plate, but the timing of syntaxis appearance and the curvature of the mountain belt did. In case of strong and/or thin overriding plates thickening of the upper plate was experienced. Near the eastern and western ends, lateral extrusion was possible. In case of weak and/or thick upper plates the original thickening was accommodated by lateral spreading, i.e. E–W elongation of the orogenic belt (BAJOLET et al. 2013, their *Figure 12*). In other words, gravity-driven secondary deformation with an E–W component was generated together with large syntaxis areas at the corners. The Pakistani greater study area lies at the western extremity of a potentially laterally extending, or extruding main Himalayan orogen.

Both lateral extrusion or a gravity-driven westwards extension of the main mountains may generate secondary E–W oriented shortening in the major syntaxial area.

Finally, based on detailed field investigations, DiPIETRO et al. (2008) interpreted the Kohistan Fault as a relatively late, post-metamorphic right-lateral transpressive fault of Oligocene age. It is noted that other authors have quite different views of Kohistan Fault as a top-north major exhumation fault (TREOLAR et al. 1992). However, the observed field indicators, structures along this fault (DiPIETRO et al. 2008) are all compatible with major and relatively late right lateral shear. On the other hand, immediately south of this fault a set of N–S trending folds can be found (*Figure 2*). In our opinion, right lateral shear along the Kohistan Fault might be compatible with generation of N–S folds arranged in echelon along a wider dextral shear zone.

5. Age constraints of the events

Timing of the main deformation events is based on three lines of evidence. Radiometric dating, including low temperature thermochronology (e.g. ZEITLER 1985, a review in TREOLAR et al. 1992); palaeomagnetic, rarely fossil or radiometric dating of molasse formations and relative sequence of events, crosscutting relations or sedimentary patterns (e.g. JOHNSON et al. 1982, 1986; GRÉLAUD et al. 2002). There are several contradicting interpretations as to the main events. According to TREOLAR et al. (1992), after the India–Kohistan island arc collision, between 50 and 40 Ma thickening and a general prograde metamorphism occurred in the overridden Indian plate margin. DiPIETRO et al. (2008) suggest a Late Cretaceous–Palaeogene (prior to 47 Ma) metamorphism. Between 40 and 30 Ma TREOLAR et al. (1992) suggest a southward (post-metamorphic) slip and internal stacking, with the Panjal Thrust at the southernmost edge of the thrust front. For both TREOLAR et al. (1992) and DiPIETRO et al. (2008) an early transversal (i.e. N–S trending) folding, doming would occur near 30 Ma (before and after 30 Ma in TREOLAR et al. 1992; prior to 31 Ma in DiPIETRO et al. 2008). From Late Oligocene onwards TREOLAR et al. (1992) propose an exhumation along Kohistan Fault with rapid cooling and synchronous re-imbrication of Indian detached units. This resulted in imbricate stacking and reverse metamorphic zonation until the Panjal Thrust. Initiation of a southern foredeep and deposition of the early molasse sediments also took place. This phase might have ended by 20 Ma. According to DiPIETRO et al. (2008) Oligocene (31 Ma) right lateral slip on Kohistan Fault occurred. For TREOLAR et al. (1992) thrusting along MBT would be later than 10 Ma; for DiPIETRO et al. (2008), the units south of Panjal Thrust should have formed progressively in Middle Miocene to Present. TREOLAR et al. (1992) suggested a Pliocene (5–2.5 Ma) growth of the Hazara and Besham antiforms. Based on low-temperature thermochronology ZEITLER (1985) suggested a 5–2 Ma growth of the Besham and Nanga Parbat syntaxes. DiPIETRO et al. (2008) proposed that even

Quaternary sediments are deformed and thus suggested ongoing uplift in the Besham dome.

GRÉLAUD *et al.* (2002) summarised the timing of deformation events of the foothills area. According to their interpretation thrusting along MBT occurred between 22 and 15 Ma, the early period of molasse deposition (concentrated mostly to the region around MBT). Between 15 and 10 Ma deformation in the NPDZ might have already begun, based on the absence of molasse of this age there. Until ca 10 Ma, during the southern deposition of Chinji Fm, no thrusting occurred along the MFT, Salt Range thrust included. Near 10 Ma the frontal Salt Range Thrust was initiated and movements continued to 5 Ma, when thrust activity decreased. However, small amount of thrusting did continue into the Quaternary (1.9 Ma). On the other hand, out of sequence thrusting was initiated and old thrusts, backthrusts were generated on the limb of the Soan syncline that grew from 5 to 1.9 Ma.

Our low temperature thermochronologic results shed some light on the timing of the Himalaya foothills deformation. Although the apatite fission track results show only partial resetting in the Margala Hills unit and therefore suggest a moderate burial of this unit beneath the Panjal Thrust, the activity along MBT should have begun before Middle Miocene, i.e. earlier than 14 Ma, thus supporting the ideas of GRÉLAUD *et al.* (2002). In the NPDZ uplift ages indicate that this zone already started to deform at Middle Miocene times again in agreement with GRÉLAUD *et al.* (2002). Fission track results from the western edge of laterally continuous Kohat Plateau (JOHNSON *et al.* 1982, MEIGS *et al.* 1994) suggest that deformation there started earlier than 8–9 Ma ago, therefore deformation along trend might be slightly diachronous.

Our 7 Ma apatite fission track ages along the northern backthrust of Soan anticline suggests that deformation at the southern edge of NPDZ imbricates should have been initiated by this time. This also means that the initiation of Soan syncline should be older than the 5 Ma proposed by GRÉLAUD *et al.* (2002).

Our apatite (U–Th)/He ages fall in the same range as earlier radiometric ages (ZEITLER 1985) for the uplifting N–S trending domal areas: the Pliocene 5–4 Ma ages suggest a quite homogenous activation of E–W shortening and resulting N–S trending folding. We also acknowledge that the real initiation of N–S trending folds could have occurred much earlier, in Oligocene, as proposed by TREOLAR *et al.* (1998) and DiPIETRO *et al.* (2008); however, as all these authors as well as ZEITLER (1985) concluded, there should be a very intense and quite young reactivation of these movements in Pliocene.

The N–S trending folds at Surghar Range do not have thermochronologic control. However, they should precede the formation of a ‘Kalabagh’ right lateral shear zone. Since this is possibly linked to thrusting over Pleistocene (e.g. GHANI *et al.* 2018), we suggest that the Pliocene event at ca 4–5 Ma could also be held responsible for the generation of these folds, east-vergent thrusts there. However, it is

also quite clear, that the N–S trending folds are carried on the back of an earlier-initiated major top-south thrust, so an alternation of N–S and E–W shortening is proposed.

Conclusions

Seismic sections in two sectors of the Himalayan foothills region: the region around Kalabagh city and the region around Islamabad suggest that there are N–S trending folds and locally east- or west-vergent thrusts that affect the Palaeozoic–Palaeogene cover of the Indian shield, as well as the Miocene–Pliocene molasse sediments.

These seismic data also suggest that the earlier proposed (KAZMI & RANA 1982, NIZAMUDDIN 1997) through-going lateral ramps, i.e. the Kalabagh and Jhelum Faults do not exist; smaller portions of these might be present, but with different orientations and nature (MCDUGALL & KHAN 1990, QAYYUM *et al.* 2015).

Map analysis also suggests that N–S trending folds are occurring in a wide area south of the Indus–Tsangpo suture (and even this main fault is re-folded by the Nanga Parbat syntaxis, BUTLER 2018). Hazara syntaxis is proposed as a major dome (cf. CALKINS & OFFIELD 1974, BOSSART *et al.* 1988, BURG & PODLADCHIKOV 1999) folding earlier main thrusts such as the Panjal Thrust and MBT (TREOLAR *et al.* 1992).

Two new alternative models were proposed for the continuation of MBT around Hazara syntaxis; one suggesting that MBT remains hidden immediately beneath the re-defined Panjal Thrust located at the contact zone of Permian volcanites and Miocene molasse; another suggesting that MBT could be continued in the Balakot Fault. We prefer the first alternative.

The NE corner of Surghar Range is proposed to be formed of relaying thrust sheets with emergent heads composed of Palaeozoic–Palaeogene and its slightly detached Miocene molasse. These relaying imbricates are taken in a southward flexure generated by a major right lateral ductile shear of a wide zone, where transpressive Riedel shears occur and where en echelon anticlines and southwards flexed earlier linear thrust faults are bent southwards (but a single, through-going Kalabagh Fault is missing).

Based on the above observations the now undulating segments of MBT and MFT, together with thrusts and overlying Miocene folds in the eastern Potwar–western Kashmir region should have been more linear (although a total linearity is not realistic). It is proposed that N–S trending folds as well as ductile flexure zones should have distorted the original more linear thrust fault/fold trend due to general (and episodic) E–W shortening. This concept is partly supported by palaeomagnetic data (KLOOTWIJK *et al.* 1981, BOSSART *et al.* 1988). If the main fault zones were more linear, the relay pattern along them suggests a left lateral shear component along MBT and a mixed, locally left, locally right lateral component along MFT.

Earlier (ZEITLER 1985) and now provided low tem-

perature thermochronological ages strongly suggest a rather general episode of E–W general shortening between 4–5 Ma for the whole northern Indian margin. However, there should have been original N–S trending dome formation eventually as early as Oligocene (DIPIETRO et al. 2008). It is also clear that longer N–S shortening and shorter E–W shortening episodes should alternate. Earthquake focal mechanisms in the study region (LISA & KHWAJA 2004, BURG et al. 2005) suggest that the region around Islamabad is mostly under E–W compression, although recent top-SW shear (along the Balakot Fault) and minor top-south shear (along the Salt Range Thrust) was also deduced from episodic GPS data (JOUANNE et al. 2014). This suggests that E–W shortening might be a consequence of main top-SSW shortening.

There are several potential explanations for generating E–W shortening and related structures in a general N–S shortening regime. Possibilities range from fault terminations of secant thrust faults in a zone (TREOLAR et al. 1992) to echelon folding along the right lateral Kohistan Fault zone of

E–W orientation. However, we speculate that E–W shortening could be much more general, suggesting a mechanism that affects the whole of Indian plate. Possibly the best explanation is given by analogue models (REPLUMAZ et al. 2012) proposing major, slightly convergent confining (lithospheric) boundaries. If applied to the northwards advance of India the converging boundaries generate secondary E–W shortening and east- or west-vergent orogens parallel to the boundaries.

Acknowledgements

MOL and Pakistani Authorities are thanked for granting permission to publish seismic sections and study data. Two anonymous reviewers are thanked for their constructive and helpful comments, suggestions. Orsolya SZTANÓ and Edit BABINSZKI are thanked for continuously encouragement and editing efforts. Their patience was instrumental in publication of the paper.

References — Irodalom

- AHMAD, S., MOHAMMAD, I. K., KHAN, A. A. & SHOUKAT, N. 2010: Himalayan-Induced Deformation and Kinematics of the Arcuate Nature of the Trans-Indus Salt Range, Northwest Himalayas, Pakistan. — Search and Discovery Article #30120 Posted June 14, 2010
- BAJOLET, F., REPLUMAZ, A. & LAINÉ, R. 2013: Orocline and syntaxes formation during subduction and collision. — *Tectonics* **32**, 1529–1546, <https://doi.org/10.1002/tect.20087>
- BOSSART, P. & OTTIGER, R. 1989: Rocks of the Murree formation in Northern Pakistan: indicators of a descending foreland basin of late Paleocene to middle Eocene age. — *Eclogae Geologicae Helvetiae* **82/1**, 133–165
- BOSSART, P., DIETRICH, D., GRECO, A., OTTIGER, R. & RAMSAY, J.G. 1988: The tectonic structure of the Hazara-Kashmir syntaxis, Southern Himalayas, Pakistan. — *Tectonics* **7/2**, 273–297, <https://doi.org/10.1029/TC007i002p00273>
- BURG, J.-P. & PODLADCHIKOV, Y. 1999: Lithospheric scale folding: numerical modelling and application to the Himalayan syntaxes. — *International Journal of Earth Sciences* **88**, 190–200. <https://doi.org/10.1007/s005310050259>
- BURG, J.-P., CÉLÉRIER, B., CHAUDHRY, N. M., GHAZANFAR, M., GNEHM, F. & SCHNELLMANN, M. 2005: Fault analysis and paleostress evolution in large strain regions: methodological and geological discussion of the southeastern Himalayan fold-and-thrust belt in Pakistan. — *Journal of Asian Earth Sciences* **24**, 445–467. <https://doi.org/10.1016/j.jseaes.2003.12.008>
- BURTNER, R. L., NIGRINI, A. & DONELICK, R. A. 1994: Thermochronology of lower Cretaceous source rocks in the Idaho-Wyoming thrust belt. — *AAPG Bulletin* **78**, 1613–1636. <https://doi.org/10.1306/a25ff233-171b-11d7-8645000102c1865d>
- BUTLER, R. W. H. 2018: Tectonic evolution of the Himalayan syntaxes: the view from Nanga Parbat. — *Geological Society of London Special Publication* 483. <https://doi.org/10.1144/sp483.5>
- CALKINS, J. A. & OFFIELD, T. W. 1974: *Geologic map of the Southern Himalaya in Hazara, Pakistan and adjacent areas, scale 1:125 000*. — Under the auspices of United States Agency of International Development, USGS, Reston Virginia; <https://doi.org/10.3133/pp716c>
- CRAIG, J., HAKHOON, N., BHAT, G. M., HAFIZ, M., KHAN, M. R., MISRA, R. & KHULLAR, S. 2018: Petroleum systems and hydrocarbon potential of the North-West Himalaya of India and Pakistan. — *Earth-Sciences Reviews* **187**, 109–185. <https://doi.org/10.1016/j.earscirev.2018.09.012>
- DANILCHIK, W. & SHAH, S. M. I. 1987: Stratigraphy and Coal Resources of the Makarwal Area, Trans-Indus Mountains, Mianwali District, Pakistan. scale 1:50 000. — *U.S. Geological Survey Professional Paper* **1341**, 38 p. <https://doi.org/10.3133/pp1341>
- DIPIETRO, J.A., AHMAD, I., HUSSAIN, A. 2008: Cenozoic kinematic history of the Kohistan fault in the Pakistan Himalaya. — *GSA Bulletin* **120/11–12**, 1428–1440. doi: 10.1130/B26204.1
- FARLEY, K. A., WOLF, R. A. & SILVER, L. T. 1996: The effects of long alpha-stopping distance on (U-Th)/He ages. — *Geochimica et Cosmochimica Acta* **60**, 4223–4229. [https://doi.org/10.1016/s0016-7037\(96\)00193-7](https://doi.org/10.1016/s0016-7037(96)00193-7)
- GALBRAITH, R. F. & LASLETT, G. M. 1993. Statistical models for mixed fission track ages.— *Nuclear Tracks and Radiation Measurements* **21**, 459–470. [https://doi.org/10.1016/1359-0189\(93\)90185-c](https://doi.org/10.1016/1359-0189(93)90185-c)
- GANSSER, A. 1964: *Geology of the Himalayas*. — Wiley Interscience, London, 289 p.
- GEE, E. R. 1980: *Geological map of the Salt Range, Pakistan, scale 1:50 000*. — Directorate of Overseas Surveys, United Kingdom, for the Government of Pakistan and the Geological Survey of Pakistan.
- GHANI, H., ZEILINGER, G., SOBEL, E. R. & HEIDARZADEH, G. 2018: Structural variation within the Himalayan fold and thrust belt: A case study from the Kohat-Potwar Fold Thrust Belt of Pakistan. — *Journal of Structural Geology*. <https://doi.org/10.1016/j.jsg.2018.07.022>

- GHAZI, S., ALI, S. H., SAGHRAEYAN, M. & HANIF, T. 2014: An overview of tectonosedimentary framework of the Salt Range, northwestern Himalayan fold and thrust belt, Pakistan. — *Arabian Journal of Geosciences* **8**, 1635–1651. <https://doi.org/10.1007/s12517-014-1284-3>
- GRÉLAUD, S., SASSI, W., FRIZON DE LAMOTTE, D., JASWAL, T. & ROURE, F. 2002: Kinematics of eastern Salt Range and South Potwar Basin (Pakistan): a new scenario. — *Marine and Petroleum Geology* **19**, 1127–1139. [https://doi.org/10.1016/s0264-8172\(02\)00121-6](https://doi.org/10.1016/s0264-8172(02)00121-6)
- JASWAL, T. M., LILLIE, R. J. & LAWRENCE, R. D. 1997: Structure and Evolution of the Northern Potwar Deformed Zone, Pakistan. — *AAPG Bulletin* **81/2**, 308–328. <https://doi.org/10.1306/522b431b-1727-11d7-8645000102c1865d>
- JADOON, I. A. K., KEMAL, A., FRISCH, W. & JASWAL, T. M. 1997: Thrust geometries and kinematics in the Himalayan foreland (North Potwar Deformed Zone), North Pakistan. — *Geologische Rundschau* **86**, 120–131. <https://doi.org/10.1130/0-8137-2328-0.275>
- JADOON, I. A. K., FRISCH, W., JASWAL, T. M. & KEMAL, A. 1999: Triangle zone in the Himalayan foreland, north Pakistan. — *Geological Society of America Special Papers* **328**, 277–286. <https://doi.org/10.1130/0-8137-2328-0.275>
- JADOON, I. A. K., HINDERER, M., WAZIR, B., YOUSAF, R., BAHADAR, S., HASSAN, M., ABBASI, Z. & JADOON, S. 2015: Structural styles, hydrocarbon prospects, and potential in the Salt Range and Potwar Plateau, north Pakistan. — *Arabian Journal of Geosciences* **8**, 5111–5125. <https://doi.org/10.1007/s12517-014-1566-9>
- JOHNSON, G. D., REYNOLDS, R. G. & BURBANK, D. W. 1986: Late Cenozoic tectonics and sedimentation in the northwestern Himalayan foredeep: Thrust ramping and associated deformation in the Potwar region. In: ALLEN, P. A. & HOMEWOOD, P. (eds): Foreland Basins. — *International Association of Sedimentologists Special Publication*, 273–291. <https://doi.org/10.1002/9781444303810.ch15>
- JOHNSON, G. D., ZEITLER, P., NAESER, C. W., JOHNSON, N. M., SUMMERS, D. M., FROST, C. D., OPDYKE, N. D. & TAHIRKHELI, R. A. K. 1982: The occurrence and fission-track ages of late Neogene and Quaternary volcanics sediments, Siwalik Group, northern Pakistan. — *Palaeogeography, Palaeoclimatology, Palaeoecology* **37**, 63–93. [https://doi.org/10.1016/0031-0182\(82\)90058-x](https://doi.org/10.1016/0031-0182(82)90058-x)
- JOUANNE, F., AWAN, A., PÉCHER, A., KAUSAR, A., MUGNIER, J. L., KHAN, N. A. & VAN MELLE, J. 2014: Present-day deformation of northern Pakistan from Salt Ranges to Karakorum Ranges. — *Journal of Geophysical Research: Solid Earth* **119**, 2487–2503. <https://doi.org/10.1002/2013JB010776>
- KAZMI, A. H. & RANA, R. A. 1982: *Tectonic map of Pakistan, scale 1:2.000.000*. — Geological Survey of Pakistan.
- KLOOTWIJK, C., NAZIRULLAH, R., DEJONG, K. & AHMED, H. 1981: A Palaeomagnetic reconnaissance of Northeastern Baluchistan, Pakistan. — *Journal of Geophysical Research* **86/B1**, 289–306. <https://doi.org/10.1029/jb086ib01p00289>
- LATIF, M. A. 1968: Geological map of SE Hazara and parts of the adjoining districts of Rawalpindi and Muzaffarabad. Scale 1 inch to 1 mile.
- LISA, M. & KHWAJA, A. A. 2004: Structural Trends and Focal Mechanism Studies in the Potwar Area with Special Emphasis on Hydrocarbon Exploration. — *Pakistan Journal of Hydrocarbon Research* **14**, 49–59.
- MARSHAK, S. 2004: Salients, Recesses, Arcs, Oroclines, and Syntaxes — A Review of Ideas Concerning the Formation of Map-view Curves in Fold-thrust Belts. — In: MCCLAY, K. R. (ed.): Thrust tectonics and hydrocarbon systems. — *AAPG Memoir* **82**, 131–156.
- MATTAUER, M. 1983: Subduction of lithosphere continentale, décollement croute manteau et chevauchements d'échelle crustale dans la chaîne de collision himalayenne. — *Comptes rendus de l'Académie des Sciences* **296/4**, 81–86.
- MCDUGALL, J. W. & KHAN, S. H. 1990: Strike-slip faulting in a foreland foldthrust belt: the Kalabagh Fault and Western Salt Range, Pakistan. — *Tectonics* **9/5**, 1061–1075. <https://doi.org/10.1029/TC009i005p101061>
- MOLNAR, P. & TAPPONIER, P. 1975: Cenozoic tectonics of Asia: Effects of a continental collision. — *Science* **189**, 419–426.
- MEIGS, A. J., BURBANK, D. W. & BECK, R. A. 1995: Middle-late Miocene (pre-10 Ma) formation of the Main Boundary thrust in the western Himalaya. — *Geology* **23/5**, 423–426. [https://doi.org/10.1130/0091-7613\(1995\)023<0423:mlmmfo>2.3.co;2](https://doi.org/10.1130/0091-7613(1995)023<0423:mlmmfo>2.3.co;2)
- NAJMAN, Y., PRINGLE, M., GODIN, L. & OLIVER, G. 2002: A reinterpretation of the Balakot Formation: Implications for the tectonics of the NW Himalaya, Pakistan. — *Tectonics* **21/5**, 1045. <https://doi.org/10.1029/2001TC001337>
- NIZAMUDDIN, M. 1997: Structural traps in the Potwar Basin, Pakistan. — *AAPG Search and Discovery, Article no # 90942, AAPG International Conf. & Exhibition, Vienna, Austria, Abstract book*.
- QAYYUM, M., SPRATT, D. A., DIXON, J. M. & LAWRENCE, R. D. 2015: Displacement transfer from fault-bend to fault-propagation fold geometry: An example from the Himalayan thrust front. — *Journal of Structural Geology* **77**, 260–276. <https://doi.org/10.1016/j.jsg.2014.10.010>
- REINERS, P. W. & BRANDON, M. T. 2006: Using thermochronology to understand orogenic erosion. — *Annual Review of Earth and Planetary Sciences* **34**, 419–466. <https://doi.org/10.1146/annurev.earth.34.031405.125202>
- REPLUMAZ, A., VIGNON, V., REGARD, V., MARTINOD, J. & GUERRERO, N. 2012: East–west shortening during north–south convergence, example of the NW Himalayan syntaxis. *Australian Journal of Geosciences* **59/6**, 845–858. <https://doi.org/10.1080/08120099.2012.701232>
- TRELOAR, P. J., COWARD, M. P., CHAMBERS, A. F., IZATT, C. N. & JACKSON, K. C. 1992: Thrust geometries, interferences and rotations in the Northwest Himalaya. — In: MCCLAY K. R. (ed.): *Thrust tectonics*. Chapman and Hall (Springer, Dordrecht), 325–342. https://doi.org/10.1007/978-94-011-3066-0_30
- WADIA, D. N. 1931: The syntaxis of the northwest Himalaya: its rocks, tectonics and orogeny. — *Records of the Geological Survey of India* **65**, 189–220.
- VESTRUM, R., DOLGOV, V., WITTMAN, G., CSONTOS, L. & GITTINS, J. 2011: 3D seismic imaging over two structurally complex surveys in the foothills of Pakistan. — *First Break* **29**, 61–70. <https://doi.org/10.3997/1365-2397.2011013>
- YEATS, R. S., KHAN, S.H. & AKHTAR, M. 1984: Late Quaternary deformation of the salt Range of Pakistan. — *Geological Society of America Bulletin* **95**, 958–966. [https://doi.org/10.1130/0016-7606\(1984\)95<958:lqdots>2.0.co;2](https://doi.org/10.1130/0016-7606(1984)95<958:lqdots>2.0.co;2)
- ZEITLER, P. K. 1985: Cooling history of the NW Himalaya. — *Tectonics* **4**, 127–151. <https://doi.org/10.1029/TC004i001p00127>